

Comparison of the Unit-Lindley and Beta Mixed Model: A Bayesian Perspective

Nirajan Bam 
Miami University
Ohio, USA

Pubudu Hitigala Kaluarachchilage 
Miami University
Ohio, USA

Abstract

Mixed-effects models are among the most extensively utilized methodologies for evaluating the relationship between correlated outcomes and covariates. The choice of model is contingent upon the nature of the outcome variable. In practical applications, it is frequently encountered that data are both correlated and constrained within the interval $(0, 1)$. The beta mixed model is typically employed to analyze such bounded and correlated data scenarios. However, recent advancements in the unit-Lindley (UL) mixed model have highlighted its advantages over the beta mixed model within a classical framework. This study introduces the UL mixed model and compares it to the beta mixed model utilizing a Bayesian approach. The STAN program was employed to conduct the Bayesian analysis and parameter estimation using Hamiltonian Monte Carlo (HMC) under the No-U-Turn Sampler (NUTS). The validity of both models was assessed through Monte Carlo Simulation. Furthermore, both models were applied to real data scenarios. Model comparison was performed using the Leave-One-Out Information Criterion (LOOIC) and the Watanabe-Akaike Information Criterion (WAIC). The results consistently indicated that the beta mixed model is superior to the UL mixed effect model in the Bayesian framework.

Keywords: unit-Lindley mixed model, beta mixed model, bounded data, rstan, HMC.

1. Introduction

In various applied fields, data scenarios like rates, proportions, and fractions are frequently encountered, which are confined between 0 and 1. These data scenarios present substantial modeling challenges attributable to the intrinsic skewness and heteroskedasticity that resist conventional correction methods (Verkuilen and Smithson 2012). Using traditional linear regression methods to examine the relationship between a bounded outcome variable and a set of covariates can violate the basic assumptions of the linear regression (Akdur 2021; Ferrari and Cribari-Neto 2004). Transformation techniques are frequently employed to rectify assumption violations; however, this approach can compromise the probabilistic characteristics inherent to the bounded nature of the outcome variables (Ferrari and Cribari-Neto 2004). Consequently, scholars have been intensively focusing on developing robust statistical models to tackle the complexities associated with data constrained within the 0 to 1 interval.

Beta regression (Ferrari and Cribari-Neto 2004) is a widely used technique for the analysis

of bounded data. Several alternative regression models have been proposed as substitutes for the traditional beta regression, particularly for modeling responses bounded within the unit interval. These alternatives differ based on whether they target the conditional mean or the conditional quantile of the response variable.

Models that focus on the conditional mean include the UL regression (Mazucheli, Menezes, and Chakraborty 2019), the generalized log-Lindley regression (Chakraborty, Ong, and Ng 2023), and the log-Bilal unit regression (Altun, El-Morshedy, and Eliwa 2021). In contrast, models that aim to estimate the conditional quantile of the response include the bounded unit-Weibull quantile regression proposed by Sapkota, Bam, and Kumar (2025), the unit-Perks quantile regression introduced by Al-Essa, Shafiq, Ozonur, and Jamal (2024), the two-parameter Burr XII quantile regression introduced by Korkmaz and Chesneau (2021), and the log-log unit quantile regression developed by (Korkmaz and Korkmaz 2023).

All of these models are limited by their underlying assumption of independent observations, rendering them unsuitable for data that exhibit correlation or clustering. In many practical applications—such as longitudinal studies or complex survey designs—the response variable may be correlated due to repeated measurements or hierarchical sampling structures. To appropriately address such dependencies in bounded response variables, mixed-effects modeling frameworks have been extended.

The UL regression model, derived from the UL distribution, is a flexible, unimodal, single-parameter distribution defined on the $(0, 1)$ interval. It belongs to the exponential family and possesses closed-form expressions for its moments and cumulative distribution function, making it particularly attractive for inference and computation. In comparison, the beta distribution—although widely used—requires two parameters and lacks closed-form expressions for its cumulative distribution and quantile functions. Similarly, the Kumaraswamy distribution, while defined on the same support, does not admit closed-form expressions for its moments. Due to these analytical and computational advantages, the UL distribution has garnered increasing attention, motivating its extension to mixed-effects models (Akdur 2021), and generalized estimating equation (Silva, Akdur, and Paula 2023) frameworks for modeling correlated bounded outcomes. Despite the simplicity of the UL model, an in-depth comparison between the beta mixed effects model and the UL mixed effects model within the Bayesian framework has not yet been conducted.

The UL mixed model, as introduced by Akdur (2021), is capable of analyzing correlated outcome variables and a set of covariates. However, the closed-form expression of the likelihood function for this model has not been derived. Consequently, parameter estimation has been dependent on numerical approximation methods. These approximation techniques rely on asymptotic properties of large sample sizes; however, as highlighted by Fong, Rue, and Wakefield (2010), there exists a paucity of rigorously established protocols to guarantee precision and accuracy in parameter estimation. Moreover, Akdur (2021) conducted a comparative analysis between the UL mixed model and the beta mixed model, elucidating the superior performance of the former relative to the latter. It remains unclear whether the superiority of the unit-Lindley model applies to all types of data situations and parameter estimation methods. While the UL mixed model has been proposed in the classical framework, there is a need for its application within a Bayesian framework, which offers greater flexibility in inference, allows for the integration of prior knowledge, and provides more robust uncertainty quantification. This gap in the literature motivates us to present a Bayesian approach to the UL mixed model and compare it with other models, such as the beta mixed model, in the context of correlated, bounded response data.

The Bayesian method for parameter estimation can effectively manage the complexity of the model (Fong *et al.* 2010). Although the classical method of parameter estimation has its own benefits, the Bayesian method offers some unique advantages over the classical approach. For instance, it allows to include prior beliefs into the model, provides straightforward parameter interpretation, and remains effective even with small sample sizes. Due to the hierarchical

nature of mixed models, the Bayesian approach was also convenient for leveraging information across different levels of the model hierarchy.

Due to the intricate nature of mixed-effects models such as the UL mixed model, obtaining a closed-form solution for the posterior distribution is challenging. As a result, employing a Markov Chain Monte Carlo (MCMC) algorithm is essential for efficiently sampling from the target posterior distribution. Some popular algorithms for this purpose are Gibbs Sampling, the Metropolis-Hastings algorithm, and Hamiltonian Monte Carlo (HMC). Among these, HMC is considered superior (Thomas and Tu 2021; Neal 2011). Therefore, HMC was considered in this study. The Bayesian programming language Stan was utilized to implement HMC. The Rstan package (Team 2023) in R (R Core Team 2024) was used for this implementation. As there were no pre-existing codes for the UL mixed model in Rstan, Stan code was created and provided in the Appendix.

The structure of the paper is as follows. Section 2 discusses the unit-Lindley distribution and its associated regression within both classical and Bayesian frameworks. Section 3 covers the beta mixed model along with its Bayesian implementation. Section 4 deals with parameter estimation and simulation. Section 5 applies the presented models to real data. Finally, Section 6 provides the discussion and conclusion.

2. Unit-Lindley (UL) distribution: Classical and Bayesian approaches

2.1. Unit-Lindley (UL) distribution and related regression

Suppose $Y \sim UL(\mu)$ is a unit-Lindley distributed random variable parameterized by its mean μ . The probability density function (PDF) of Y is given by:

$$f(y) = \frac{(1 - \mu)^2}{\mu(1 - y)^3} \exp\left(-\frac{y(1 - \mu)}{\mu(1 - y)}\right), \quad (1)$$

where y and μ are bounded within the interval of 0 and 1 (Mazucheli *et al.* 2019). Assume Y_1, \dots, Y_n are independent random variables such that $Y_i \sim UL(\mu_i)$, where μ_i denotes the mean parameter. Let \mathbf{x}_i be the covariate vector associated with the i -th observation. The regression model formulated to estimate the conditional mean of the outcome variable is given as:

$$\psi(\mu_i) = \mathbf{x}_i^T \boldsymbol{\delta}, \quad (2)$$

where, $\boldsymbol{\delta} = (\delta_1, \delta_2, \dots, \delta_p)^T$ is a vector of unknown parameters, and $\mathbf{x}_i^T = (x_{i1}, \dots, x_{ip})$ is a vector of known covariates. The application of the link function, $\psi(\mu_i) = \log\left(\frac{\mu_i}{1 - \mu_i}\right)$, guarantees that the fitted value of conditional mean of the outcome variable remains confined within the interval (0,1) (Akdur 2021). Other link functions—such as log-log, complementary log-log, and probit—can also be employed where appropriate. Model presented in equation (2) is not capable to accommodate correlated or clustered responses. Thus, mixed-effects model is required when response variable is correlated or clustered in nature.

2.2. Unit-Lindley (UL) mixed-effects model

As discussed earlier, the UL model shows limited capability in modeling situations involving longitudinal data or clustered data situations. In these cases, it is crucial to use models that can incorporate both random and fixed effects. Generalized linear mixed models (GLMMs) are well-suited for handling both fixed and random effects simultaneously within a single model. The application of generalized linear mixed models (GLMMs) requires the outcome variable's distribution to be part of the natural exponential family (Petterle, Taconeli, da Silva, da Silva, Laureano, and Bonat 2023). While the UL distribution is included in the broader exponential

family (Mazucheli *et al.* 2019), it is not classified within the natural exponential family. Several studies (Bonat, Ribeiro, and Zeviani 2015; Pettele *et al.* 2023) have employed methodologies similar to those used in generalized linear mixed models (GLMMs), including the classical UL mixed model (Akdur 2021), to analyze data with correlated and clustered bounded outcome variables. Thus, the approach of the generalized mixed-effects model is extended for this study.

Define y_{ij} as the bounded response for the j -th outcome ($j \in \{1, 2, \dots, n_i\}$) of the i -th subject ($i \in \{1, \dots, n\}$), with y_{ij} being distributed according to the UL distribution. The conditional mean of y_{ij} is associated with the linear predictors via the link function $\psi(\cdot)$,

$$\psi(\mu_{ij}) = x_{ij}^T \boldsymbol{\delta} + z_{ij}^T \mathbf{u}_i, \quad (3)$$

where $\psi(\cdot)$ is the logit link function, $\boldsymbol{\delta}$ is the vector of regression coefficients of the fixed effect of known covariates of x_{ij} and \mathbf{u}_i is the random effect vector of random effect design vector z_{ij} . Following is the conditional probability density function of outcome variable, conditioned on random effect.

$$f(y_i | \mathbf{u}_i) = \prod_{j=1}^{n_i} \frac{(1 - \mu_{ij})^2}{\mu_{ij}(1 - y_{ij})^3} \exp\left(-\frac{y_{ij}(1 - \mu_{ij})}{\mu_{ij}(1 - y_{ij})}\right), \quad (4)$$

where μ_{ij} is related to fixed and random effects through logit link function.

In this research, we utilize a random intercept UL model, which results in the design matrix for the random effect being an identity matrix. Thus, following is the mathematical form of the UL random effect model;

$$\text{logit}(\mu_{ij}) = x_{ij}^T \boldsymbol{\delta} + u_i. \quad (5)$$

$$\mu_{ij} = \frac{\exp(x_{ij}^T \boldsymbol{\delta} + u_i)}{1 + \exp(x_{ij}^T \boldsymbol{\delta} + u_i)}. \quad (6)$$

Distribution of random effect term $u_i \sim N(0, \sigma_u^2)$.

In Bayesian approach, the prior distribution holds significant importance as it incorporates prior beliefs or evidence into the analysis. Existing literature has commonly employed a multivariate normal prior for the fixed effects and an inverse gamma prior for the variance component of random effect in both linear and nonlinear mixed-effects models (Hobert and Casella 1996; Lachos, Bandyopadhyay, and Dey 2011; Lachos, Castro, and Dey 2013; Mohsenkhani, Mohhammadzadeh, and Baghfalaki 2019). These priors are not only widely used but also known to be conditionally conjugate (Hobert and Casella 1996). In the augmented beta mixed model, Mohsenkhani *et al.* (2019) applied a multivariate normal prior for the fixed effects and an inverse gamma prior for the variance component of random effect. Thus, the prior distributions assumed for the unknown parameters of this model are: $\boldsymbol{\delta} \sim N(0, \Sigma_\delta)$, $\sigma_u^2 \sim I\Gamma(\alpha, \beta)$. At this point, the UL mixed-effect model under Bayesian framework can be specified as follows;

$$\begin{aligned} y_{ij} | u_i &\sim UL(\mu_{ij}) \\ u_i &\sim N(0, \sigma_u^2) \\ \text{logit}(\mu_{ij}) &= x_{ij}^T \boldsymbol{\delta} + u_i. \end{aligned}$$

Let $\boldsymbol{\eta} = (\boldsymbol{\delta}, u_i, \sigma_u^2)$ denote the vector comprising mutually independent parameters of interest. The conditional likelihood function for the outcome vector \mathbf{y} is defined as,

$$\mathcal{L}(\boldsymbol{\eta}; \mathbf{y}, \mathbf{x}, \mathbf{u}) = \prod_{i=1}^n f(y_i | u_i) = \prod_{i=1}^n \prod_{j=1}^{n_i} \frac{(1 - \mu_{ij})^2}{\mu_{ij}(1 - y_{ij})^3} \exp\left(-\frac{y_{ij}(1 - \mu_{ij})}{\mu_{ij}(1 - y_{ij})}\right) \quad (7)$$

Consequently, the joint posterior distribution can be expressed as

$$\pi(\boldsymbol{\eta}, \mathbf{u} | \mathbf{y}, \mathbf{x}) \propto \mathcal{L}(\boldsymbol{\eta} | \mathbf{y}, \mathbf{x}, \mathbf{u}) \pi(\boldsymbol{\delta}) \pi(\mathbf{u} | \sigma_u^2) \pi(\sigma_u^2). \quad (8)$$

Hyper-parameter $\Sigma_\delta = \sigma_\delta^2 I_p, \sigma_\delta^2 = 100$ (Mohsenkhani *et al.* 2019). Based on sensitivity analysis using the `powersense` package in R, along with model comparison using the Leave-One-Out Information Criterion (LOOIC) and the Widely Applicable Information Criterion (WAIC), the optimal hyperparameter set was selected from among three alternative prior specifications. Lower values of LOOIC and WAIC indicate better model fit. Among the three candidates, **Prior Set A** was selected in 75.6% of the simulations based on LOOIC and in 80.6% based on WAIC. Summary statistics from 500 replications for LOOIC and WAIC are presented in Tables 1 and 2, respectively. In addition, the sensitivity analysis results shown in Table 3 indicate that Prior Set A is less sensitive compared to the other prior sets. Based on the combined evidence from LOOIC, WAIC, and sensitivity analysis, Prior Set A was selected.

The three alternative prior sets considered in the analysis are listed below:

- **Prior A:** $\sigma_u^2 \sim \text{IG}(0.1, 1)$; $\delta \sim N(0, \Sigma_\delta)$, $\Sigma_\delta = \sigma_\delta^2 I_p$ with $\sigma_\delta^2 = 100$
- **Prior B:** $\sigma_u^2 \sim \text{IG}(0.01, 0.01)$; $\delta \sim N(0, \Sigma_\delta)$, $\Sigma_\delta = \sigma_\delta^2 I_p$ with $\sigma_\delta^2 = 100$
- **Prior C:** $\sigma_u^2 \sim \text{IG}(0.1, 0.1)$; $\delta \sim N(0, \Sigma_\delta)$, $\Sigma_\delta = \sigma_\delta^2 I_p$ with $\sigma_\delta^2 = 1$

Table 1: Summary of LOOIC simulation results

Summary measure	Prior A	Prior B	Prior C
Min	-191.24	-190.32	-190.97
1st Quartile	-124.99	-123.85	-124.83
Median	-108.44	-105.88	-107.09
Mean	-108.87	-100.85	-106.85
3rd Quartile	-89.30	-79.52	-86.36
Max	-43.62	-10.44	-34.43
Best Prior %	75.6%	6.4%	18.00%

Table 2: Summary of WAIC simulation results

Summary measure	Model 1	Model 2	Model 3
Min	-192.22	-191.47	-191.90
1st Quartile	-126.08	-125.13	-125.90
Median	-109.68	-106.99	-108.20
Mean	-110.08	-102.06	-108.00
3rd Quartile	-90.36	-81.01	-87.70
Max	-45.57	-10.99	-35.60
Best Prior %	80.6%	5.2%	14.2%

Markov Chain Monte Carlo (MCMC) was employed for posterior distribution sampling and parameter estimation. Gibbs sampling, the Metropolis-Hastings (MH) algorithm, and HMC are popular algorithms for MCMC. HMC offers distinct advantages over alternative methods (Thomas and Tu 2021). In addition, the full conditional distributions of the parameters do not have known closed-form expressions, making Gibbs sampling unsuitable for this study. Consequently, this study implemented HMC via the Rstan package in R. A closed-form expression of the joint posterior distribution is not achievable. Therefore, we relied on MCMC methods to explore the posterior behavior, as theoretical derivation is not feasible. Specifically, we examined how the chosen priors influenced the posterior distributions using posterior predictive plots and various convergence diagnostics, including effective sample size, Gelman-Rubin diagnostic, autocorrelation function (ACF) plots, and trace plots, as described in Section 4

Table 3: Sensitivity analysis for different prior sets for UL mixed-effects model

Prior set	Parameters	Prior	Likelihood	Diagnosis
A	δ_1	0.0210	0.0526	
	δ_2	0.0118	0.0557	
	δ_3	0.0126	0.0575	
	δ_4	0.0224	0.0556	
	σ_u^2	0.0500	0.0577	
B	δ_1	0.0135	0.0857	
	δ_2	0.0114	0.0863	
	δ_3	0.0204	0.0846	
	δ_4	0.0173	0.0853	
	σ_u^2	1.270	0.0103	Strong prior/Weak likelihood
C	δ_1	0.0924	0.0224	Strong Prior/ Weak likelihood
	δ_2	0.0126	0.0805	
	δ_3	0.0080	0.0674	
	δ_4	0.0371	0.0541	
	σ_u^2	0.3320	0.0925	Strong prior/ Weak likelihood

This study is based exclusively on the logit link function. However, other link functions—such as probit, log-log, and complementary log-log—were also tested and showed satisfactory performance. Alternative link functions may be adopted as needed, depending on the application context.

3. Beta mixed-effects model with Bayesian implementation

As discussed earlier, beta regression (Ferrari and Cribari-Neto 2004) is a widely used method to analyze bounded response variables in conjunction with a set of covariates. The regression model introduced by Ferrari and Cribari-Neto (2004) relies on the following reparametrized density function of the beta distribution.

$$f(y|\mu, \phi) = \frac{\Gamma(\phi)}{\Gamma(\phi\mu)\Gamma(1-y)\phi} y^{(\phi\mu-1)}(1-y)^{(1-\mu)\phi-1}, \quad 0 < y < 1, \quad 0 < \mu < 1, \quad \phi > 0. \quad (9)$$

In this case, random variable Y follows beta distribution with parameters $\phi\mu$ and $\phi(1-y)$, where mean is μ and variance is $\frac{\mu(1-\mu)}{(1+\phi)}$.

Consider a set of beta random variables $\{Y_{ij}\}$, where i and j range over $i = 1, 2, \dots, n$ and $j = 1, 2, \dots, n_i$, respectively. Assume y_i is a vector representing the responses for all measurements of subject i and u_i denote the random effect for subject i . The following relation delineates the beta mixed-effects model:

$$\psi(\mu_{ij}) = \text{logit}(\mu_{ij}) = x_{ij}^T \boldsymbol{\delta} + z_{ij}^T u_i, \quad (10)$$

where $\psi(\cdot)$ is the link function, $\boldsymbol{\delta}$ is the regression coefficients of the fixed effect x_{ij} , u_i is the random effect vector of the random effect design vector z_{ij} . The distribution of random effect u_i is normal with mean 0 and variance σ_u^2 . In this study, we adopt a random intercept model, thereby rendering the random-effects design matrix as an identity matrix. Following is beta random intercept model;

$$\text{logit}(\mu_{ij}) = x_{ij}^T \boldsymbol{\delta} + u_i \quad (11)$$

$$\mu_{ij} = \frac{\exp(x_{ij}^T \boldsymbol{\delta} + u_i)}{1 + \exp(x_{ij}^T \boldsymbol{\delta} + u_i)}. \quad (12)$$

In Bayesian approach, the prior distribution holds significant importance as it incorporates prior beliefs or evidence into the analysis. Following a thorough review of contemporary studies (Hobert and Casella 1996; Lachos *et al.* 2013; Mohsenkhani *et al.* 2019), we have used following priors for each parameter: $\boldsymbol{\delta} \sim N(\mathbf{0}, \Sigma_\delta)$, $\sigma_u^2 \sim IG(\alpha_1, \beta_1)$, $\phi \sim \Gamma(\alpha_1, \beta_1)$. These priors were also used by Mohsenkhani *et al.* (2019) in the context of augmented beta mixed effects model. Now the Bayesian beta mixed-effects model can be specified as follows;

$$\begin{aligned} y_{ij}|u_i &\sim \text{beta}(\mu_{ij}\phi, (1 - \mu_{ij})\phi) \\ u_i &\sim N(0, \sigma_u^2) \\ \text{logit}(\mu_{ij}) &= x_{ij}^T \boldsymbol{\delta} + u_i \end{aligned}$$

Let $\boldsymbol{\eta} = (\delta, u_i, \sigma_u^2, \phi)$ denote the vector comprising mutually independent parameters of interest. The conditional likelihood function of the outcome vector \mathbf{y} is given by:

$$\mathcal{L}(\boldsymbol{\eta}; \mathbf{y}, \mathbf{x}, \mathbf{u}) = \prod_{i=1}^n \prod_{j=1}^{n_i} f(y_{ij}|\mu_{ij}, \phi) = \prod_{i=1}^n \prod_{j=1}^{n_i} \frac{\Gamma(\phi)}{\Gamma(\phi\mu_{ij})\Gamma(1 - y_{ij})\phi} y^{(\phi\mu_{ij}-1)}(1 - y_{ij})^{(1-\mu_{ij})\phi-1}. \quad (13)$$

Then, the joint posterior distribution is given by

$$\pi(\boldsymbol{\eta}, \mathbf{u}|\mathbf{y}, \mathbf{x}) \propto \mathcal{L}(\boldsymbol{\eta}|\mathbf{y}, \mathbf{x}, \mathbf{u})\pi(\boldsymbol{\eta})\pi(\mathbf{u}|\sigma_u^2)\pi(\sigma_u^2)\pi(\phi). \quad (14)$$

Hyper-parameter $\Sigma_\delta = \sigma_\delta^2 I_p$, $\sigma_\delta^2 = 100$ (Mohsenkhani *et al.* 2019). To select the hyperparameters, model comparison criteria—WAIC and LOOIC—were applied alongside a sensitivity analysis using the `powersense` package in R. Summary results based on 500 replications for LOOIC and WAIC are presented in Tables 4 and 5, respectively. Based on the simulation results, **Prior Set A** was selected in 73.8% of the cases according to LOOIC and 78.2% of the cases according to WAIC. In addition, the selected prior set exhibited lower sensitivity compared to the other three sets of priors; detailed results are provided in Table 6. Following four alternative prior specifications were considered:

- **Prior A:** $\sigma_u^2 \sim IG(0.1, 1)$; $\boldsymbol{\delta} \sim N(0, \Sigma_\delta)$, $\Sigma_\delta = \sigma_\delta^2 I_p$ with $\sigma_\delta^2 = 100$; $\Phi \sim G(0.01, 0.01)$
- **Prior B:** $\sigma_u^2 \sim IG(0.1, 0.1)$; $\boldsymbol{\delta} \sim N(0, \Sigma_\delta)$, $\Sigma_\delta = \sigma_\delta^2 I_p$ with $\sigma_\delta^2 = 1$; $\Phi \sim G(0.01, 0.01)$
- **Prior C:** $\sigma_u^2 \sim IG(0.01, 0.01)$; $\boldsymbol{\delta} \sim N(0, \Sigma_\delta)$, $\Sigma_\delta = \sigma_\delta^2 I_p$ with $\sigma_\delta^2 = 100$; $\Phi \sim G(0.01, 0.01)$
- **Prior D:** $\sigma_u^2 \sim IG(0.01, 1)$; $\boldsymbol{\delta} \sim N(0, \Sigma_\delta)$, $\Sigma_\delta = \sigma_\delta^2 I_p$ with $\sigma_\delta^2 = 1$; $\Phi \sim G(1, 1)$

Table 4: Summary of LOOIC simulation results

Summary measure	Prior A	Prior B	Prior C	Prior D
Min	-278.39	-278.16	-278.12	-275.82
1st Quartile	-154.67	-154.46	-153.22	-152.62
Median	-137.32	-136.00	-131.75	-135.24
Mean	-140.57	-139.39	-128.95	-138.57
3rd Quartile	-121.44	-120.39	-103.64	-119.55
Max	-81.41	-72.73	-15.38	-79.81
Best Prior %	73.8%	19.6%	6.00%	0.6%

Table 5: Summary of WAIC simulation results

Summary measure	Prior A	Prior B	Prior C	Prior D
Min	-279.13	-279.04	-278.85	-276.44
1st Quartile	-155.49	-155.08	-153.95	-153.09
Median	-137.88	-136.89	-132.61	-135.72
Mean	-141.25	-140.04	-129.56	-139.11
3rd Quartile	-122.02	-120.93	-104.16	-120.05
Max	-81.84	-73.31	-15.45	-80.24
Best Prior %	78.2%	15.4%%	6.40%	0.00%

Table 6: Sensitivity analysis for different prior sets for beta mixed-effects model

Prior set	Parameters	Prior	Likelihood	Diagnosis
A	δ_1	0.0199	0.0440	
	δ_2	0.0090	0.0519	
	δ_3	0.0134	0.0529	
	δ_4	0.0179	0.0464	
	σ^2	0.0500	0.0624	
	Φ	0.0500	0.0170	
B	δ_1	0.0907	0.0421	Strong prior/Weak likelihood
	δ_2	0.0095	0.0732	
	δ_3	0.0178	0.0826	
	δ_4	0.0550	0.0703	Prior data conflict
	σ^2	0.0550	0.0505	Strong prior/Weak likelihood
	Φ	0.0531	0.1210	Prior data conflict
C	δ_1	0.0250	0.0787	
	δ_2	0.0183	0.0878	
	δ_3	0.0170	0.0813	
	δ_4	0.0233	0.0757	
	σ^2	1.2400	0.0115	Strong prior/weak likelihood
	Φ	0.0730	0.0983	Prior data conflict
D	δ_1	0.0239	0.0817	
	δ_2	0.0077	0.0722	
	δ_3	0.0159	0.0825	
	δ_4	0.0220	0.0757	
	σ^2	0.0523	0.0974	Prior data conflict
	Φ	0.0462	0.3240	Prior data conflict

The MCMC techniques were utilized to draw samples from the target posterior distribution to estimate the model parameters. In particular, HMC was implemented using the Rstan package in R. The beta mixed-effects model itself is not a new contribution; however, the corresponding Stan code and its implementation are presented independently in this paper for comparison purposes.

4. Parameter estimation and simulation

4.1. Parameter estimation

As discussed in preceding sections, the MCMC was proposed for parameter estimation. Owing to the convenience and myriad potential advantages associated with HMC, this technique was employed for the generation of samples from the posterior distribution and for the estimation of parameters. For instance, Gibbs sampling requires the full conditional distribution of each parameter, while Metropolis-Hastings requires a large number of iterations, and the convergence rate is slower when using a randomly proposed proposal distribution. HMC doesn't rely on the full conditional distribution and utilizes a guided proposal distribution. Extensive mathematical derivations and algorithmic descriptions for HMC can be found in the reference provided by Neal (2011). In HMC, the utilization of the gradient of the logarithm of the posterior aids in favoring samples from regions with higher density, resulting in a faster convergence rate compared to other algorithms (Thomas and Tu 2021). While HMC predominantly samples from regions of high posterior density, it also adeptly captures samples from the tail areas of the distribution. Despite the numerous advantages of HMC over alternative methods, its mathematical framework is considerably more complex. In HMC, the goal is to efficiently explore the posterior distribution of model parameters by treating them as particles in a physical system. The Hamiltonian equations describe how the particles' positions (parameters) and momentum (movement) evolve over time. HMC uses these equations to guide the sampler through the parameter space, allowing for more efficient exploration of high-probability regions of the posterior distribution. To solve these equations Euler's equations can be used but these methods accumulated errors after a large number of steps (Neal 2011). Thus, Leapfrog method is preferred over simpler methods like Euler's because it better preserves the system's energy and avoids the accumulation of numerical errors, leading to more stable and accurate trajectories (Thomas and Tu 2021). This makes leapfrog particularly effective for efficiently exploring the parameter space.

The speed at which HMC converges depends on the chosen leapfrog step size and the number of leapfrog steps (L). As elucidated by Hoffman and Gelman (2014), an insufficiently small value of L induces erratic random walk behavior in HMC; conversely, an excessively large value of L demands substantial computational resources. To address this issue with HMC, Hoffman and Gelman (2014) introduced the No-U-Turn Sampler (NUTS), which autonomously determines an appropriate leapfrog size without external intervention. Although NUTS addresses the automatic selection of the step size L in HMC, the method struggles with discrete parameters. HMC relies on numerical solutions to differential equations, which are ineffective for discontinuous functions, making convergence unreliable when the parameter has a discontinuous density (Hernández, Vergara, Valdenegro-Toro, and Jorquera 2020). Since the parameter space of our proposed model is continuous, this drawback does not apply, and HMC remains the superior method compared to the other two for our study. To implement HMC in our study, we used Stan, an R package that incorporates NUTS, an adaptive variant of HMC. Since the model is novel and no existing Stan code was available, we developed custom Stan code for both models and used it in R to estimate the parameters.

4.2. Convergence assessment

Assessing convergence is a critical step in MCMC to verify that the chain has thoroughly explored the target distribution. This ensures that the samples are representative of the posterior, allowing for reliable parameter estimates and minimizing the risk of biased results due to insufficient sampling. Owing to its accelerated convergence rates, HMC necessitated fewer MCMC iterations relative to the other two algorithms. Accordingly, this investigation employed 10,000 iterations, with 50% allocated as a warm up sample. Convergence was appraised utilizing trace plots, autocorrelation function (ACF) plots, Gelman-Rubin diagnostic

plots. Effective convergence of the chain is confirmed when the trace plot stabilizes around the average. The ACF plot helps in determining the rate of convergence; high autocorrelation indicates slower convergence, while low autocorrelation indicates faster convergence. The Gelman-Rubin diagnostic is useful for checking convergence when multiple chains are run in parallel with different starting points. A Gelman-Rubin statistic (\hat{R}) close to 1 indicates good convergence. The high effective sample sizes (100 times per chain) and close-to-unity \hat{R} values indicate reliable estimation and convergence of the MCMC sampling process, enhancing confidence in the validity of the statistical analyses and conclusions drawn from the study (Vehtari, Gelman, Simpson, Carpenter, and Bürkner 2021). Evaluating the Monte Carlo error (MCE) is imperative for assessing the variability attributable to simulation. The MCE was computed using the standard deviation of the posterior draws for each parameter, as provided by RStan. Finally, to evaluate the precision of parameter recovery in the simulation, root mean square error (RMSE) and Bias were utilized.

In HMC sampling, diagnostics such as step size, leapfrog steps, tree depth, and energy provide insight into the efficiency and reliability of the sampling process. The step size, tuned during warm-up, controls how far the sampler moves at each step—smaller values improve accuracy but may require more steps. The number of leapfrog steps reflects the detail of the simulated trajectory, with excessively high values increasing computational cost. Tree depth, used in the NUTS algorithm, indicates trajectory complexity, while the energy diagnostic helps assess whether the sampler is exploring the posterior efficiently. In our models, these diagnostics remained within acceptable ranges, supporting the validity of the sampling process.

4.3. Bayesian model comparison

Several criterion are commonly used in Bayesian model comparison, but two widely accepted ones are the LOOIC and WAIC. LOOIC and WAIC are fully Bayesian criterion accessible through the ‘loo’ package in R, making them popular choices for model comparison in various studies. LOOIC is rigorously derived from the leave-one-out cross-validation (LOOCV) methodology, offering a robust evaluation of predictive accuracy for out-of-sample data.

$$\text{LOOIC} = -2 \sum_{i=1}^n \log(L_{p(i)}(y_i)), \quad (15)$$

where $L_{p(i)}$ denotes the log posterior density of the i -th observation (Vehtari, Gelman, and Gabry 2017). A smaller value of LOOIC indicates a better fit of the model. WAIC was introduced by Watanabe in 2010 (Watanabe and Opper 2010) on (DIC). It is computed using the following relationship:

$$\text{WAIC} = -2(\text{elpd}_{\text{waic}}) + 2\text{pwaic}. \quad (16)$$

Here, $\text{elpd}_{\text{waic}}$ represents the expected logarithmic pointwise predictive density, which quantifies how well the model predicts each individual data point, averaging over all observations. The pwaic represents the effective number of parameters, which adjusts for model complexity. It accounts for the effective "degrees of freedom" used by the model, penalizing overfitting by incorporating the variance of the posterior distribution. A smaller value of WAIC indicates a better model fit. It offers a good trade-off between the complexity and goodness-of-fit of the model. loo package in R was used to extract WAIC. The default settings of the loo package were used without any modifications.

4.4. Simulation

The performance of the model was evaluated using Monte Carlo simulation. The parameter values and covariate distributions utilized in this simulation were adopted from those employed by Akdur (2021). The simulation was conducted using R. The number of subjects simulated in this study was denoted by n and the measurements per subject by n_i . The parameter

recovery simulation of UL mixed model was conducted based on the data generated by setting parameter values; $\delta_0 = -0.3, \delta_1 = -0.6, \delta_2 = 0.7, \delta_3 = 0.1, \delta_4 = 0.2$, and $\sigma_u^2 = 1$ (Akdur 2021). The sample sizes varied, including 10, 20, 30, and 40, with the measurements per subject set at 10 and 15. The UL mixed-effects model in this simulation has the following form:

$$\pi(\mu_{ij}) = \log\left(\frac{\mu_{ij}}{1 - \mu_{ij}}\right) = \delta_0 + \delta_1 x_{1ij} + \delta_2 x_{2ij} + \delta_3 x_{3ij} + \delta_4 x_{4ij} b_i, \quad (17)$$

$$i = 1, 2, \dots, n \text{ and } j = 1, 2, \dots, n_i.$$

Distribution of covariates were $x_{1ij} \sim Unif(-1, 1)$, $x_{2ij} \sim N(0, 1)$, $x_{3ij} \sim N(0, 1)$, $x_{4ij} \sim Unif(0, 1)$, $b_i \sim N(0, \sigma_b^2)$. To sample data for a unit Lindley random variable, the following quantile function was employed:

$$Q(u|\text{par}) = \frac{1 + \text{par} + W_- \left((1 + \text{par})e^{-(1+\text{par})}(u-1) \right)}{1 + W_- \left((1 + \text{par})e^{-(1+\text{par})}(u-1) \right)},$$

$$u \sim Unif(0, 1).$$

Here, W_- is negative branch of Lambert function, and "par" ($\text{par} > 0$) represents parameter of unit-Lindley distribution.

Similar parameter values, covariate distributions, and sample sizes were defined to generate data for the beta mixed model. Response variable was generated according to beta distribution by using "rbeta" function in R. Additionally, the beta distribution requires a precision parameter, which was set to 10. For both models Bias and RMSE were used to evaluate the simulated parameter's accuracy.

4.5. Evaluation of misspecification in UL and beta mixed-effects models

The primary focus of this paper is to present the UL mixed-effects model and compare it with the beta mixed-effects model within a Bayesian framework. Thus, we have carefully selected priors and adhered to all assumptions to ensure correctly specified models. However, to raise practitioners' awareness, we also present a set of brief scenarios in which models may be misspecified and illustrate the potential consequences of such misspecification through simulation studies. In mixed-effects models, random effects are treated as latent variables. Following standard practice, we assume they follow a normal distribution. However, in real-world data, this assumption may not hold—random effects may exhibit skewness or heavier tails. If the true distribution of the random effects deviates from normality, this misspecification can lead to biased estimates for parameters that depend on the random effects. To illustrate this issue, we generated data based on all the scenarios presented in Section 4.4, except for the distribution of the random effects. Specifically, we assumed that the random effects followed a skew-normal distribution with a skewness parameter $\lambda = 1, 2$ and variance $\sigma_u^2 = 1$. We considered two settings: one with a sample size of $n = 10$ and 10 measurements per subject, and another with $n = 20$ and 15 measurements per subject. The results of the misspecification simulation are presented in Tables 7, 9, 8, 10, 11, 12, 13, and 14. As expected, the results indicate that when the true distribution of the random effects deviates from normality—such as following a skew-normal distribution—parameter estimates become biased. The degree of bias increases with the level of skewness. Compared to the UL mixed-effects model, the beta mixed-effects model exhibits less bias under misspecification of the random intercept distribution.

Table 7: Simulation results: misspecified UL mixed-effects model with skew-normal random effect ($n = 10, n_i = 10, \lambda = 1$)

Parameter	True	Mean	2.5%	97.5 %	Bias	MSE
δ_0	-0.3000	1.3218	0.7245	1.9182	1.6218	2.7781
δ_1	-0.6000	-0.6036	-0.8767	-0.3301	-0.0036	0.0168
δ_2	0.7000	0.7043	0.5444	0.8645	0.0043	0.0071
δ_3	0.1000	0.0974	-0.0617	0.2567	-0.0026	0.0068
δ_4	0.2000	0.1899	-0.3563	0.7359	-0.0101	0.0816
σ_u^2	1.0000	1.3818	0.6660	2.7254	0.3818	0.6246

Table 8: Simulation results: misspecified UL mixed-effects model with skew-normal random effect ($n = 20, n_i = 15, \lambda = 1$)

Parameter	True	Mean	2.5%	97.5%	Bias	MSE
δ_0	-0.3000	1.3037	0.9068	1.7008	1.6037	2.6535
δ_1	-0.6000	-0.6035	-0.7549	-0.4522	-0.0035	0.0059
δ_2	0.7000	0.7010	0.6126	0.7896	0.0010	0.0023
δ_3	0.1000	0.1028	0.0154	0.1901	0.0028	0.0022
δ_4	0.2000	0.2061	-0.0956	0.5083	0.0061	0.0236
σ_u^2	1.0000	1.3402	0.8273	2.1348	0.3402	0.3088

Table 9: Simulation results: misspecified UL mixed-effects model with skew-normal random effect ($n = 10, n_i = 10, \lambda = 2$)

Parameter	True	Mean	2.5%	97.5%	Bias	MSE
δ_0	-0.3000	2.1239	1.3775	2.8704	2.4239	6.1184
δ_1	-0.6000	-0.6051	-0.8762	-0.3338	-0.0051	0.0166
δ_2	0.7000	0.7045	0.5463	0.8629	0.0045	0.0068
δ_3	0.1000	0.0976	-0.0600	0.2554	-0.0024	0.0066
δ_4	0.2000	0.1910	-0.3497	0.7310	-0.0090	0.0791
σ_u^2	1.0000	2.5033	1.2481	4.8570	1.5033	3.8882

Table 10: Simulation results: misspecified UL mixed-effects model with skew-normal random effect ($n = 20, n_i = 15, \lambda = 2$)

Parameter	True	Mean	2.5%	97.5%	Bias	MSE
δ_0	-0.3000	2.0977	1.5904	2.6054	2.3977	5.8900
δ_1	-0.6000	-0.6039	-0.7536	-0.4540	-0.0039	0.0057
δ_2	0.7000	0.7012	0.6139	0.7887	0.0012	0.0023
δ_3	0.1000	0.1028	0.0163	0.1893	0.0028	0.0021
δ_4	0.2000	0.2068	-0.0921	0.5060	0.0068	0.0231
σ_u^2	1.0000	2.4311	1.5240	3.8356	1.4311	2.7246

Table 11: Simulation results: misspecified beta mixed-effects model with skew-normal random effect ($n = 10, n_i = 10, \lambda = 1$)

Parameter	True	Mean	2.5%	97.5%	Bias	MSE
δ_0	-0.3000	1.2260	0.6487	1.8113	1.5260	2.4761
δ_1	-0.6000	-0.5887	-0.8609	-0.3150	0.0113	0.0176
δ_2	0.7000	0.6912	0.5259	0.8555	-0.0088	0.0062
δ_3	0.1000	0.0946	-0.0616	0.2507	-0.0054	0.0063
δ_4	0.2000	0.2164	-0.3218	0.7552	0.0164	0.0809
σ_u^2	1.0000	1.0945	0.5122	2.1861	0.0945	0.5329

Table 12: Simulation results: misspecified beta mixed-effects model with skew-normal random effect ($n = 20, n_i = 15, \lambda = 1$)

Parameter	True	Mean	2.5%	97.5%	Bias	MSE
δ_0	-0.3000	1.2144	0.8304	1.6010	1.5144	2.3618
δ_1	-0.6000	-0.5956	-0.7455	-0.4451	0.0044	0.0060
δ_2	0.7000	0.6896	0.5983	0.7805	-0.0104	0.0025
δ_3	0.1000	0.1019	0.0159	0.1877	0.0019	0.0017
δ_4	0.2000	0.1922	-0.1035	0.4876	-0.0078	0.0236
σ_u^2	1.0000	0.8257	0.5040	1.3245	-0.1743	0.4890

Table 13: Simulation results: misspecified beta mixed-effects model with skew-normal random effect ($n = 10, n_i = 10, \lambda = 2$)

Parameter	True	Mean	2.5%	97.5%	Bias	MSE
δ_0	-0.3000	1.9402	1.2064	2.6883	2.2402	5.1295
δ_1	-0.6000	-0.4668	-0.7613	-0.1699	0.1332	0.0721
δ_2	0.7000	0.6521	0.4757	0.8270	-0.0479	0.0047
δ_3	0.1000	0.0701	-0.0948	0.2353	-0.0299	0.0055
δ_4	0.2000	0.0879	-0.4790	0.6485	-0.1121	0.0408
σ_u^2	1.0000	2.2431	1.0724	4.4188	1.2431	1.7452

Table 14: Simulation results: misspecified beta mixed-effects model with skew-normal random effect ($n = 20, n_i = 15, \lambda = 2$)

Parameter	True	Mean	2.5%	97.5%	Bias	MSE
δ_0	-0.3000	1.9728	1.5112	2.4394	2.2728	5.2655
δ_1	-0.6000	-0.5532	-0.7158	-0.3897	0.0468	0.0085
δ_2	0.7000	0.6447	0.5456	0.7428	-0.0553	0.0059
δ_3	0.1000	0.0973	0.0047	0.1898	-0.0027	0.0023
δ_4	0.2000	0.1797	-0.1413	0.5004	-0.0203	0.0246
σ_u^2	1.0000	1.8584	1.1406	2.9687	0.8584	1.0463

In addition to the normality assumption of the random effect term, having too few categories in a random effect can lead to biased parameter estimates. For instance, if a variable such as sex has only two categories and is included as a random effect, there is insufficient variability to reliably estimate the between-group variance. To illustrate this issue, we simulated data based on the schemes described in Section 4.4. Specifically, we considered sample sizes of 10 and 20, with two measurements per subject. Simulation results presented in Tables 15 and

16 indicate that the UL mixed effects model produces biased variance estimates. A similar pattern is observed for the beta mixed model, as shown in Tables 17 and 18.

Table 15: Beta mixed effects model simulation results with $n = 10$ subjects and $n_i = 2$ measurements per subject

Parameter	True	Mean	2.5%	97.5%	Bias	MSE
δ_0	-0.3000	-0.2428	-1.1989	0.7462	0.0572	0.4127
δ_1	-0.6000	-0.5806	-1.4023	0.2440	0.0194	0.2820
δ_2	0.7000	0.6931	0.1935	1.1927	-0.0069	0.1110
δ_3	0.1000	0.0466	-0.4474	0.5424	-0.0534	0.1151
δ_4	0.2000	0.2749	-1.3761	1.9206	0.0749	1.1537
σ_u^2	1.0000	0.4606	0.1398	1.2344	-0.5394	0.4330

Table 16: UL mixed effects model simulation results with $n = 20$ subjects and $n_i = 2$ measurements per subject

Parameter	True	Mean	2.5%	97.5%	Bias	MSE
δ_0	-0.3000	-0.1109	-0.7057	0.4946	0.1891	0.2675
δ_1	-0.6000	-0.6405	-1.1498	-0.1315	-0.0405	0.1407
δ_2	0.7000	0.7093	0.4074	1.0122	0.0093	0.0468
δ_3	0.1000	0.0875	-0.2124	0.3871	-0.0125	0.0398
δ_4	0.2000	0.2273	-0.7845	1.2408	0.0273	0.5680
σ_u^2	1.0000	0.2311	0.0855	0.5463	-0.7689	0.6140

Table 17: Beta mixed effects model simulation results with $n = 10$ subjects and $n_i = 2$ measurements per subject

Parameter	True	Mean	2.5%	97.5%	Bias	MSE
δ_0	-0.3000	-0.2923	-1.2646	0.6800	0.0077	0.3178
δ_1	-0.6000	-0.5375	-1.3845	0.3144	0.0625	0.1832
δ_2	0.7000	0.6697	0.1502	1.1947	-0.0303	0.0698
δ_3	0.1000	0.0908	-0.4122	0.5949	-0.0092	0.0763
δ_4	0.2000	0.2177	-1.4526	1.8808	0.0177	0.8208
σ_u^2	1.0000	0.3367	0.1056	1.0320	-0.6633	0.4471

Table 18: Beta mixed effects model simulation results with $n = 20$ subjects and $n_i = 2$ measurements per subject

Parameter	True	Mean	2.5%	97.5%	Bias	MSE
δ_0	-0.3000	-0.2626	-0.9139	0.3872	0.0374	0.1705
δ_1	-0.6000	-0.5403	-1.1113	0.0307	0.0597	0.0910
δ_2	0.7000	0.5968	0.2533	0.9452	-0.1032	0.0460
δ_3	0.1000	0.0794	-0.2518	0.4110	-0.0206	0.0267
δ_4	0.2000	0.1706	-0.9536	1.2925	-0.0294	0.4193
σ_u^2	1.0000	0.1233	0.0611	0.2517	-0.8767	0.7687

Moreover, mixed effects models typically assume that fixed effects and random effects are independent and uncorrelated. However, a high correlation between these two components can lead to biased parameter estimates. To illustrate this issue, we generated correlated random effects and fixed-effect covariates. The simulation scenarios follow those described in Section 4.4, except we introduced correlation between the random effects and the fixed-effect

covariates x_{i2} and x_{i3} . We considered two settings: one with a sample size of $n = 10$ and 10 measurements per subject, and another with $n = 20$ and 15 measurements per subject. Simulation results for the UL mixed effects model with correlated random and fixed effects are presented in Tables 19 and 20, while the results for the beta mixed effects model are shown in Tables 21 and 22. The results indicate that the estimates of certain fixed effects parameters, particularly δ_2 and δ_3 , are biased. Moreover, the magnitude of bias is greater in the UL mixed effects model compared to the beta mixed effects model.

Table 19: Simulation results for the UL mixed effects model with correlated random and fixed effects ($n = 10, n_i = 10$)

Parameter	True	Mean	X2.5.	X97.5.	Bias	MSE
δ_0	-0.3000	-0.2158	-0.7059	0.2759	0.0842	0.0386
δ_1	-0.6000	-0.5851	-0.8781	-0.2915	0.0149	0.0243
δ_2	0.7000	0.7771	0.6059	0.9473	0.0771	0.0139
δ_3	0.1000	0.3854	0.0354	0.7297	0.2854	0.1189
δ_4	0.2000	0.1866	-0.3971	0.7705	-0.0134	0.1065
σ_u^2	1.0000	0.6696	0.2612	1.4655	-0.3304	0.1545

Table 20: Simulation results for the UL mixed effects model with correlated random and fixed effects ($n = 20, n_i = 15$)

Parameter	True	Mean	X2.5.	X97.5.	Bias	MSE
δ_0	-0.3000	-0.1734	-0.4929	0.1471	0.1266	0.0256
δ_1	-0.6000	-0.5935	-0.7533	-0.4337	0.0065	0.0078
δ_2	0.7000	0.7557	0.6603	0.8511	0.0557	0.0057
δ_3	0.1000	0.2930	0.0996	0.4866	0.1930	0.0481
δ_4	0.2000	0.2098	-0.1102	0.5306	0.0098	0.0294
σ_u^2	1.0000	0.7074	0.3843	1.2111	-0.2926	0.1047

Table 21: Simulation results for the beta mixed effects model with correlated random and fixed effects ($n = 10, n_i = 10$)

Parameter	True	Mean	X2.5.	X97.5.	Bias	MSE
δ_0	-0.3000	-0.3095	-0.7860	0.1649	-0.0095	0.0914
δ_1	-0.6000	-0.5931	-0.8562	-0.3284	0.0069	0.0209
δ_2	0.7000	0.7541	0.5925	0.9184	0.0541	0.0100
δ_3	0.1000	0.3572	0.0437	0.6791	0.2572	0.0971
δ_4	0.2000	0.2029	-0.3162	0.7205	0.0029	0.0621
σ_u^2	1.0000	0.7074	0.2660	1.5547	-0.2926	0.1857

Table 22: Simulation results for the beta mixed effects model with correlated random and fixed effects ($n = 20, n_i = 15$)

Parameter	True	Mean	X2.5.	X97.5.	Bias	MSE
δ_0	-0.3000	-0.2924	-0.6097	0.0239	0.0076	0.0467
δ_1	-0.6000	-0.5928	-0.7382	-0.4468	0.0072	0.0055
δ_2	0.7000	0.7321	0.6427	0.8221	0.0321	0.0032
δ_3	0.1000	0.2579	0.0838	0.4351	0.1579	0.0324
δ_4	0.2000	0.1838	-0.1050	0.4717	-0.0162	0.0193
σ_u^2	1.0000	0.7646	0.4223	1.2949	-0.2354	0.1261

4.6. Simulation results under correct model specification

Before starting the simulation, we assessed the potential for convergence issues in the model. We ensured that all chains were mixing well, with \hat{R} values close to 1 and no significant autocorrelation. Additionally, we confirmed that the effective sample size was greater than 10% of the total sample size, indicating sufficient sampling efficiency. With these checks met, we proceeded with the simulation. The simulation results for the UL mixed model are presented in Table 23. These results indicate that all parameters were accurately recovered, with the 95% credible intervals capturing the true parameters. The biases for the fixed effects terms ranged from 0 to 0.0184, and the RMSEs for these terms ranged from 0.0331 to 0.3570. For the variance of the random effects, the biases ranged from 0.0201 to 0.1176, while the RMSEs ranged from 0.1747 to 0.5172. Furthermore, all Gelman-Rubin statistics (\hat{R}) were between 1 and 1.002. As the sample size increases, the 95% credible intervals become narrower for all parameters, indicating greater precision in the estimates. Additionally, RMSE decreases with larger sample sizes. The bias also reduces as the number of repeated measurements per subject increases.

The simulation results for the beta mixed model are presented in Table 24. These results indicate that all parameters were accurately recovered, and the 95% credible intervals captured the true parameters. The biases for the fixed effects terms ranged from 0.0002 to 0.0151, and the RMSEs for these terms ranged from 0.0308 to 0.3378. For the variance of the random effects, the absolute biases ranged from 0.0064 to 0.1200, while the RMSEs ranged from 0.2347 to 0.5174. Furthermore, all Gelman-Rubin statistics (\hat{R}) were between 1. Similar trends in bias, RMSE, and the 95% credible interval were observed in the simulation results for the beta mixed model, as in the UL mixed model.

5. Application of presented models

5.1. Analysis of child mortality rates in South Asian nations

The child mortality rate constitutes a pivotal indicator for evaluating the Human Development Index (HDI), rendering it a prevalent variable in diverse research domains. Despite the worldwide reduction in child mortality rates, pronounced disparities endure between developed and developing nations (Zakaria, Tahir, and Iftikhar Ul Husnain 2020). A significant proportion of South Asian countries fall under the developing category, with this region accounting for one-third of global child mortality (Zakaria *et al.* 2020). Consequently, this study investigated the child mortality rates and their associated determinants within South Asian countries. Considering the longitudinal nature of the child mortality rate data in the South Asian region, which ranges between 0 and 1, the UL mixed model and the beta mixed model offer suitable approaches for analysis. Data for this application were obtained from the World Bank (The World Bank 2020). Due to data unavailability in certain countries within the South Asian region, our analysis excludes Bhutan and Afghanistan. The mortality rate of children was quantified as deaths per thousands births. The time frame spans from the year 2000 (the base year) to 2020. The predictor variables of child mortality rates include time, health expenditure, the Human Development Index (HDI), and average years of schooling. Time represents the year in which the child mortality rate is observed, ranging from 2000 (treated as 0) to 2020 (treated as 20). Health expenditure refers to the country's spending on health per person. The HDI, an indicator ranging from 0 to 1, reflects a country's performance in health, education, and income. The average years of schooling represent the mean number of years of education completed. Figure 1 presents a time plot that shows trends in mortality rate of children over time across countries in the South Asia over time. The results of the child mortality analysis are presented in Table 26. Convergence was assessed using trace plots, pairs plots, ACF plots, and the Gelman and Rubin diagnostic (\hat{R}). All plots verified adequate convergence. Trace plots of parameter estimates for child mortality data using the UL mixed

Table 23: Parameter recovery simulation of unit-Lindley mixed-effects model

n	n_i	Parameters	True	Mean	Bias	RMSE	Merror	2.5%	97.5%	\hat{R}	
10	10	δ_0	-0.3	-0.3015	-0.0015	0.357	0.0026	-0.5423	-0.0434	1.002	
	10	δ_1	-0.6	-0.6040	-0.0040	0.1486	0.0004	-0.7154	-0.4870	1.000	
	10	δ_2	0.7	0.7003	0.0003	0.0892	0.0002	0.6315	0.7645	1.000	
	10	δ_3	0.1	0.0943	-0.0057	0.0909	0.0002	0.0344	0.1660	1.000	
	10	δ_4	0.2	0.1948	-0.0052	0.2934	0.0009	-0.0284	0.4269	1.000	
	10	σ_u^2	1.0	1.0251	0.0251	0.5172	0.0029	0.6660	1.3257	1.001	
	15	δ_0	-0.3	-0.3165	-0.0165	0.2001	0.0026	-0.5423	-0.0434	1.002	
	15	δ_1	-0.6	-0.6004	-0.0004	0.0851	0.0004	-0.7154	-0.4870	1.000	
	15	δ_2	0.7	0.7030	0.0030	0.0511	0.0002	0.6315	0.7645	1.000	
	15	δ_3	0.1	0.0985	-0.0015	0.0505	0.0002	0.0344	0.1660	1.000	
	15	δ_4	0.2	0.2082	0.0082	0.1666	0.0009	-0.0284	0.4269	1.000	
	15	σ_u^2	1.0	1.1059	0.1059	0.3022	0.0029	0.6660	1.3257	1.001	
	20	10	δ_0	-0.3	-0.2925	0.0075	0.2575	0.0026	-0.5423	-0.0434	1.002
		10	δ_1	-0.6	-0.5985	0.0015	0.1067	0.0004	-0.7154	-0.4870	1.000
		10	δ_2	0.7	0.6958	-0.0042	0.0643	0.0002	0.6315	0.7645	1.000
10		δ_3	0.1	0.1018	0.0018	0.0612	0.0002	0.0344	0.1660	1.000	
10		δ_4	0.2	0.2066	0.0066	0.2115	0.0009	-0.0284	0.4269	1.000	
10		σ_u^2	1.0	0.9015	-0.0985	0.3655	0.0029	0.6660	1.3257	1.001	
15		δ_0	-0.3	-0.2963	0.0037	0.2309	0.0026	-0.5423	-0.0434	1.002	
15		δ_1	-0.6	-0.5998	0.0002	0.0838	0.0004	-0.7154	-0.4870	1.000	
15		δ_2	0.7	0.7011	0.0011	0.0485	0.0002	0.6315	0.7645	1.000	
15		δ_3	0.1	0.0974	-0.0026	0.0488	0.0002	0.0344	0.166	1.000	
15		δ_4	0.2	0.1898	-0.0102	0.1676	0.0009	-0.0284	0.4269	1.000	
15		σ_u^2	1.0	0.9799	-0.0201	0.3513	0.0029	0.6660	1.3257	1.001	
30		10	δ_0	-0.3	-0.2816	0.0184	0.2001	0.0026	-0.5423	-0.0434	1.002
		10	δ_1	-0.6	-0.6023	-0.0023	0.0851	0.0004	-0.7154	-0.4870	1.000
		10	δ_2	0.7	0.6966	-0.0034	0.0511	0.0002	0.6315	0.7645	1.000
	10	δ_3	0.1	0.1022	0.0022	0.0505	0.0002	0.0344	0.1660	1.000	
	10	δ_4	0.2	0.2024	0.0024	0.1666	0.0009	-0.0284	0.4269	1.000	
	10	σ_u^2	1.0	0.8986	-0.1014	0.3022	0.0029	0.6660	1.3257	1.001	
	15	δ_0	-0.3	-0.2974	0.0026	0.1934	0.0026	-0.5423	-0.0434	1.002	
	15	δ_1	-0.6	-0.6021	-0.0021	0.0668	0.0004	-0.7154	-0.4870	1.000	
	15	δ_2	0.7	0.7007	0.0007	0.0403	0.0002	0.6315	0.7645	1.000	
	15	δ_3	0.1	0.0987	-0.0013	0.039	0.0002	0.0344	0.1660	1.000	
	15	δ_4	0.2	0.2078	0.0078	0.135	0.0009	-0.0284	0.4269	1.000	
	15	σ_u^2	1.0	0.9448	-0.0552	0.289	0.0029	0.6660	1.3257	1.001	
	40	10	δ_0	-0.3	-0.2853	0.0147	0.1806	0.0026	-0.5423	-0.0434	1.002
		10	δ_1	-0.6	-0.5972	0.0028	0.0694	0.0004	-0.7154	-0.4870	1.000
		10	δ_2	0.7	0.6984	-0.0016	0.0447	0.0002	0.6315	0.7645	1.000
10		δ_3	0.1	0.1000	0.0000	0.0423	0.0002	0.0344	0.1660	1.000	
10		δ_4	0.2	0.2003	0.0003	0.1499	0.0009	-0.0284	0.4269	1.000	
10		σ_u^2	1.0	0.8824	-0.1176	0.2706	0.0029	0.6660	1.3257	1.001	
15		δ_0	-0.3	-0.2926	0.0074	0.1747	0.0026	-0.5423	-0.0434	1.002	
15		δ_1	-0.6	-0.6012	-0.0012	0.0575	0.0004	-0.7154	-0.4870	1.000	
15		δ_2	0.7	0.698	-0.002	0.0354	0.0002	0.6315	0.7645	1.000	
15		δ_3	0.1	0.1003	0.0003	0.0331	0.0002	0.0344	0.1660	1.000	
15		δ_4	0.2	0.1993	-0.0007	0.1207	0.0009	-0.0284	0.4269	1.000	
15		σ_u^2	1.0	0.9454	-0.0546	0.2419	0.0029	0.6660	1.3257	1.001	

Table 24: Parameter recovery simulation of beta mixed-effects model

n	n_i	Parameters	True	Mean	Bias	RMSE	Mcerror	2.5%	97.5%	\hat{R}
10	10	δ_0	-0.3	-0.3154	-0.0154	0.3378	0.0042	-0.8432	0.2106	1.001
	10	δ_1	-0.6	-0.5975	0.0025	0.1231	0.0011	-0.8473	-0.3469	0.9999
	10	δ_2	0.7	0.6994	-0.0006	0.0779	0.0007	0.5456	0.8538	1.000
	10	δ_3	0.1	0.0981	-0.0019	0.0700	0.0006	-0.0462	0.2425	1.0004
	10	δ_4	0.2	0.2002	0.0002	0.2454	0.0024	-0.2948	0.6949	1.0001
	10	σ_u^2	1.0	1.0565	0.0565	0.5174	0.0058	0.4972	2.1067	1.0002
	10	ϕ	10	10.032	0.0324	1.6328	0.0145	7.2460	13.268	1.0002
15	15	δ_0	-0.3	-0.3117	-0.0117	0.1912	0.0043	-0.8231	0.1983	1.000
	15	δ_1	-0.6	-0.5900	0.0100	0.0716	0.0009	-0.7881	-0.3914	1.000
	15	δ_2	0.7	0.7027	0.0027	0.0437	0.0005	0.5813	0.8246	1.0002
	15	δ_3	0.1	0.0983	-0.0017	0.0396	0.0005	-0.0151	0.2119	1.0004
	15	δ_4	0.2	0.2046	0.0046	0.1416	0.0018	-0.1868	0.5960	1.0005
	15	σ_u^2	1.0	1.1200	0.1200	0.2922	0.0061	0.5481	2.1927	0.9998
	15	ϕ	10	10.097	0.0977	0.9037	0.0112	7.8509	12.625	0.0006
20	10	δ_0	-0.3	-0.3009	-0.0009	0.2431	0.0034	-0.6579	0.0550	1.0004
	10	δ_1	-0.6	-0.5951	0.0049	0.0869	0.0007	-0.7689	-0.4210	1.0001
	10	δ_2	0.7	0.6897	-0.0103	0.0556	0.0005	0.5830	0.7966	1.000
	10	δ_3	0.1	0.0971	-0.0029	0.0498	0.0004	-0.0025	0.1969	1.0003
	10	δ_4	0.2	0.1977	-0.0023	0.1748	0.0016	-0.1462	0.5418	1.0006
	10	σ_u^2	1.0	0.9336	-0.0664	0.3444	0.004	0.5519	1.5244	1.0002
	10	ϕ	10	9.793	-0.2070	1.0778	0.0096	7.8200	11.983	0.9999
	15	δ_0	-0.3	-0.3027	-0.0027	0.2232	0.0038	-0.6477	0.0416	1.000
	15	δ_1	-0.6	-0.5971	0.0029	0.073	0.0006	-0.7357	-0.4582	1.0003
	15	δ_2	0.7	0.6954	-0.0046	0.0427	0.0004	0.6103	0.7808	1.0003
	15	δ_3	0.1	0.0984	-0.0016	0.0388	0.0003	0.0188	0.1779	1.0002
	15	δ_4	0.2	0.1973	-0.0027	0.1338	0.0013	-0.0766	0.4712	1.0004
	15	σ_u^2	1.0	0.9932	-0.0068	0.3332	0.0045	0.6055	1.5949	1.0001
	15	ϕ	10	9.888	-0.1113	0.8611	0.0077	8.3059	11.609	1.0002
30	10	δ_0	-0.3	-0.2854	0.0146	0.1912	0.0029	-0.5756	0.0046	1.0004
	10	δ_1	-0.6	-0.5874	0.0126	0.0716	0.0006	-0.7287	-0.4457	1.0003
	10	δ_2	0.7	0.6918	-0.0082	0.0437	0.0003	0.6049	0.7787	1.0005
	10	δ_3	0.1	0.0963	-0.0037	0.0396	0.0003	0.0150	0.1775	1.0001
	10	δ_4	0.2	0.1919	-0.0081	0.1416	0.0012	-0.0877	0.4715	0.9997
	10	σ_u^2	1.0	0.9221	-0.0779	0.2922	0.0032	0.6029	1.3777	1.0002
	10	ϕ	10	9.690	-0.3095	0.9037	0.0074	8.0776	11.445	1.0003
	15	δ_0	-0.3	-0.2972	0.0028	0.1858	0.0033	-0.5749	-0.0198	1.0004
	15	δ_1	-0.6	-0.5948	0.0052	0.0585	0.0005	-0.7077	-0.4817	0.9999
	15	δ_2	0.7	0.693	-0.007	0.0367	0.0003	0.6237	0.7624	1.0001
	15	δ_3	0.1	0.1015	0.0015	0.0330	0.0003	0.0370	0.1661	1.0002
	15	δ_4	0.2	0.1957	-0.0043	0.1126	0.0010	-0.0273	0.4186	1.0003
	15	σ_u^2	1.0	0.9562	-0.0438	0.2791	0.0037	0.6401	1.4074	1.0005
	15	ϕ	10	9.798	-0.2013	0.7268	0.0058	8.5086	11.180	1.0002
40	10	δ_0	-0.3	-0.2937	0.0063	0.1655	0.0025	-0.5432	-0.0444	1.000
	10	δ_1	-0.6	-0.5849	0.0151	0.0626	0.0005	-0.7073	-0.4624	1.0001
	10	δ_2	0.7	0.6899	-0.0101	0.0399	0.0003	0.6148	0.7652	0.9999
	10	δ_3	0.1	0.0961	-0.0039	0.0349	0.0003	0.0260	0.1662	1.0001
	10	δ_4	0.2	0.1936	-0.0064	0.1212	0.0010	-0.0483	0.4353	1.000
	10	σ_u^2	1.0	0.903	-0.0907	0.2551	0.0027	0.6258	1.2801	1.0001
	10	ϕ	10	9.6176	-0.3824	0.8546	0.0061	8.2232	11.118	1.0001
	15	δ_0	-0.3	-0.2968	0.0032	0.1669	0.0030	-0.5374	-0.0566	1.0003
	15	δ_1	-0.6	-0.5929	0.0071	0.0493	0.0004	-0.6905	-0.4950	1.0002
	15	δ_2	0.7	0.6949	-0.0051	0.0308	0.0002	0.6350	0.7550	1.0002
	15	δ_3	0.1	0.0990	-0.0010	0.0283	0.0002	0.0432	0.1549	1.0003
	15	δ_4	0.2	0.1981	-0.0019	0.1024	0.0008	0.0050	0.3910	1.0001
	15	σ_u^2	1.0	0.9579	-0.0421	0.2347	0.0032	0.6781	1.3384	1.0002
	15	ϕ	10	9.7821	-0.02179	0.6362	0.0048	8.6606	10.971	1.0003

model are depicted in Figure 2, while those for the beta mixed model are shown in Figure 3. ACF plots of the UL mixed model are presented in Figure 4, while those for the beta mixed model are presented in Figure 5. All statistics for Gelman and Rubin diagnostics were approximately 1 (see Table 26). All chains converged well, with zero divergences recorded (see Table 25). The tree depths for all chains were below 10, and the number of leapfrog steps remained below 200 for Model 1 and below 400 for Model 2. Additionally, all acceptance statistics exceeded 90%, indicating good sampling efficiency. Based on LOOIC and WAIC (see Table 26), the beta mixed model outperforms the UL mixed model. Posterior predictive checks were also used to compare how well the posterior predictive samples matched the original data. Posterior predictive check (PPC) box plots for the posterior predictive samples and the observed data from both the UL and beta mixed models are presented in Figure 6. The PPC box plots from the beta mixed model more closely resemble the observed data, suggesting that the beta mixed model provides a more accurate and reliable fit to the data than the UL mixed model. This improvement is not only statistically significant but also practically meaningful, indicating that the beta mixed model better captures key features of the data that are relevant for inference and prediction in this context. Based on the mean of the estimated parameters (refer to Table 26), both models demonstrated a negative association between child mortality rates and predictors: time, health expenditure, years of schooling and HDI. Based on the findings of this study, the key message for policymakers in South Asia is to maintain strong investments in education, healthcare spending, and human development initiatives, as these are critical to sustaining and accelerating the decline in child mortality rates.

Table 25: Summary of convergence diagnostics

Model	Chain	Accept Stat	Step Size	Tree Depth	# of Leapfrog	Divergences	Energy
Model 1	All Chains	0.9437	0.0352	6.53	117.63	0	-271.23
	Chain 1	0.9370	0.0376	6.39	110.92	0	-271.23
	Chain 2	0.9407	0.0365	6.48	114.40	0	-271.38
	Chain 3	0.9402	0.0362	6.48	115.01	0	-271.17
	Chain 4	0.9568	0.0303	6.74	130.01	0	-271.11
Model 2	All Chains	0.9354	0.0155	7.51	273.80	0	-472.40
	Chain 1	0.9269	0.0165	7.43	255.46	0	-472.37
	Chain 2	0.9473	0.0138	7.65	308.47	0	-472.39
	Chain 3	0.9317	0.0161	7.47	264.35	0	-472.63
	Chain 4	0.9357	0.0156	7.47	267.17	0	-472.38

Table 26: Parameter estimates and comparative analysis of beta and unit-Lindley mixed-effects models for child mortality rate data

Models	Parameters	mean	SE	SD	2.50%	97.50%	n_eff	\hat{R}	WAIC	LOOIC
Model 1	δ_0	0.2660	0.0173	1.3813	-2.4887	2.9235	6392	1.001	-558.8	-558.8
	δ_1	-0.0031	0.0002	0.0206	-0.0444	0.0369	10943	1.000		
	δ_2	-0.0009	0.0000	0.0008	-0.0025	0.0007	15602	1.000		
	δ_3	-0.0615	0.0012	0.1079	-0.2766	0.1484	8359	1.001		
	δ_4	-5.0886	0.0397	3.1391	-11.1547	1.2291	6266	1.002		
	σ_u^2	0.3325	0.0020	0.1985	0.1208	0.8470	10341	1.001		
Model 2	δ_0	-1.1190	0.0053	0.4429	-1.9927	-0.2539	6935	1.000	-981.9	-979.9
	δ_1	-0.0206	0.0001	0.0062	-0.0328	-0.0084	8263	1.001		
	δ_2	-0.0011	0.0000	0.0002	-0.0015	-0.0006	17023	1.000		
	δ_3	-0.0372	0.0004	0.0418	-0.1183	0.0462	11698	1.001		
	δ_4	-2.6554	0.0081	0.7898	-4.2459	-1.1304	9526	1.000		
	σ_u^2	0.4030	0.0025	0.2255	0.1540	0.9744	8167	1.000		

Note: Model 1 is the unit-Lindley mixed model, Model 2 is the beta mixed model. δ_0 , δ_1 , δ_2 , δ_3 , and δ_4 represent the fixed effects for intercept, time, health expenditure, schooling, and HDI, respectively. σ_u^2 is the variance of the random intercept. The 2.5% and 97.5% columns denote the lower and upper limits of the 95% credible interval. n_eff is the effective sample size, and \hat{R} is the Gelman and Rubin diagnostic statistic.

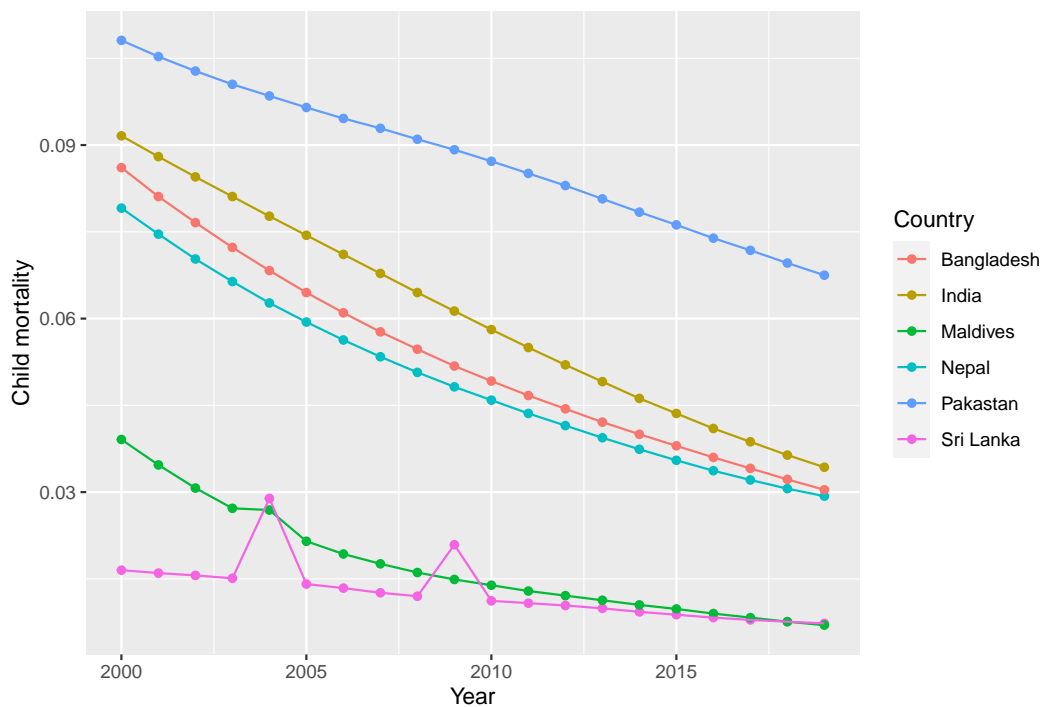


Figure 1: Time plot of mortality rates of children across South Asian countries over time

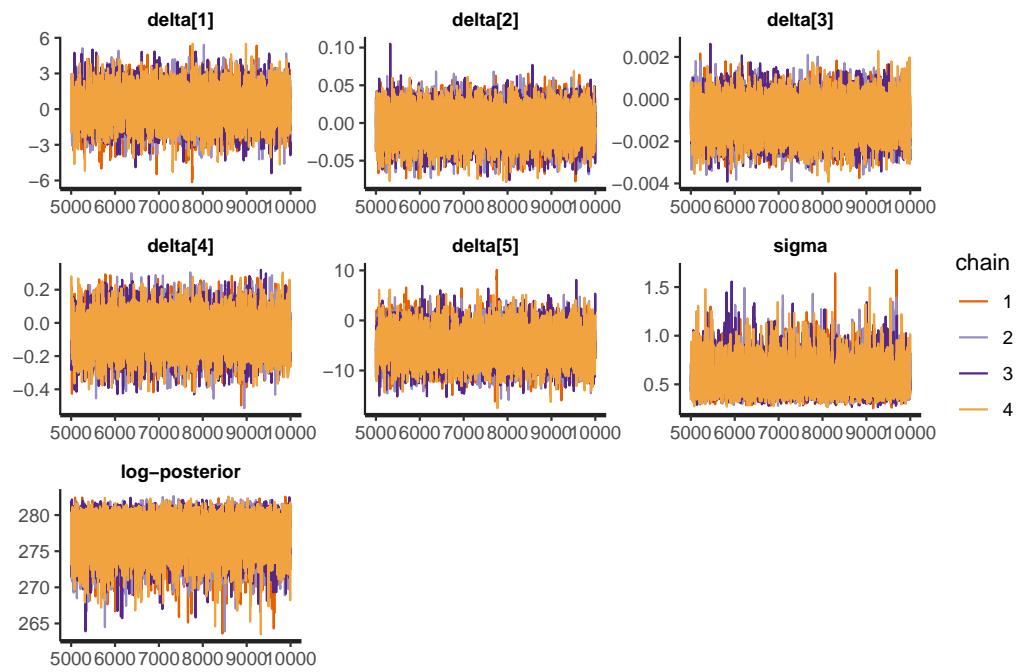


Figure 2: Trace plot of parameter estimates for child mortality data using a UL mixed model

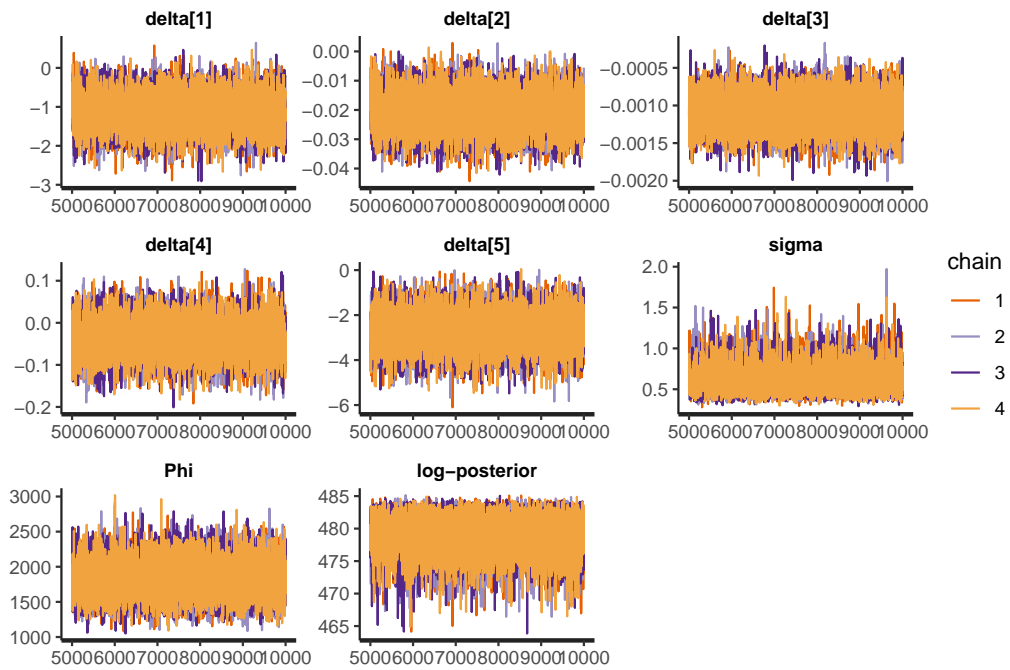


Figure 3: Trace plot of parameter estimates for child mortality data using a beta mixed model

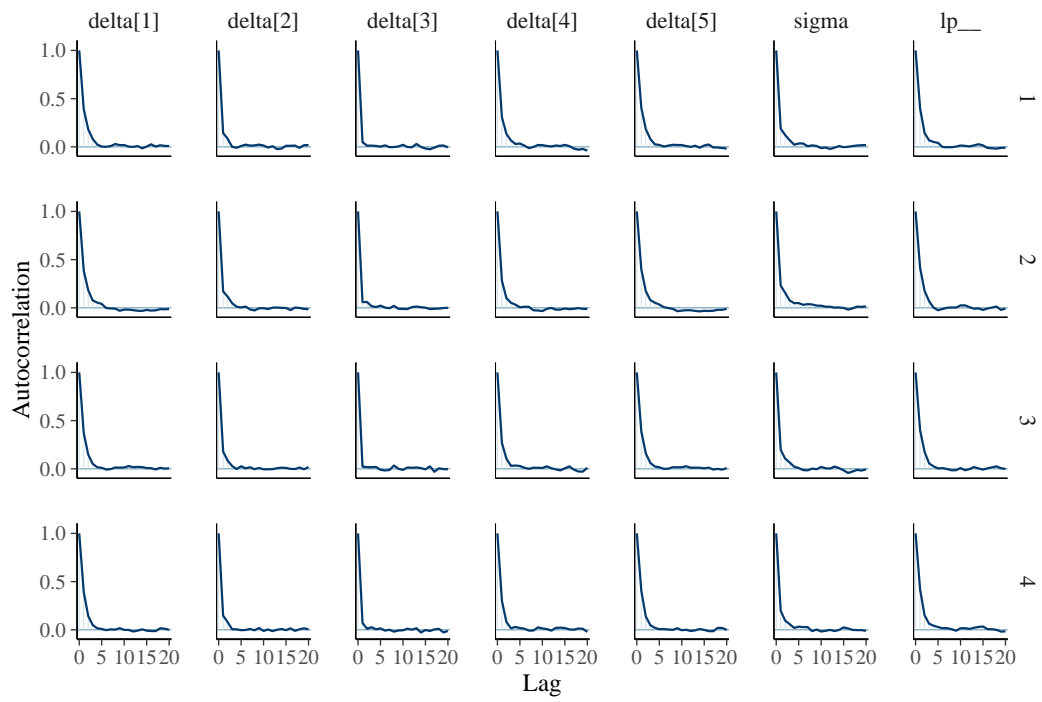


Figure 4: ACF plot of parameter estimates for child mortality data using a UL mixed model

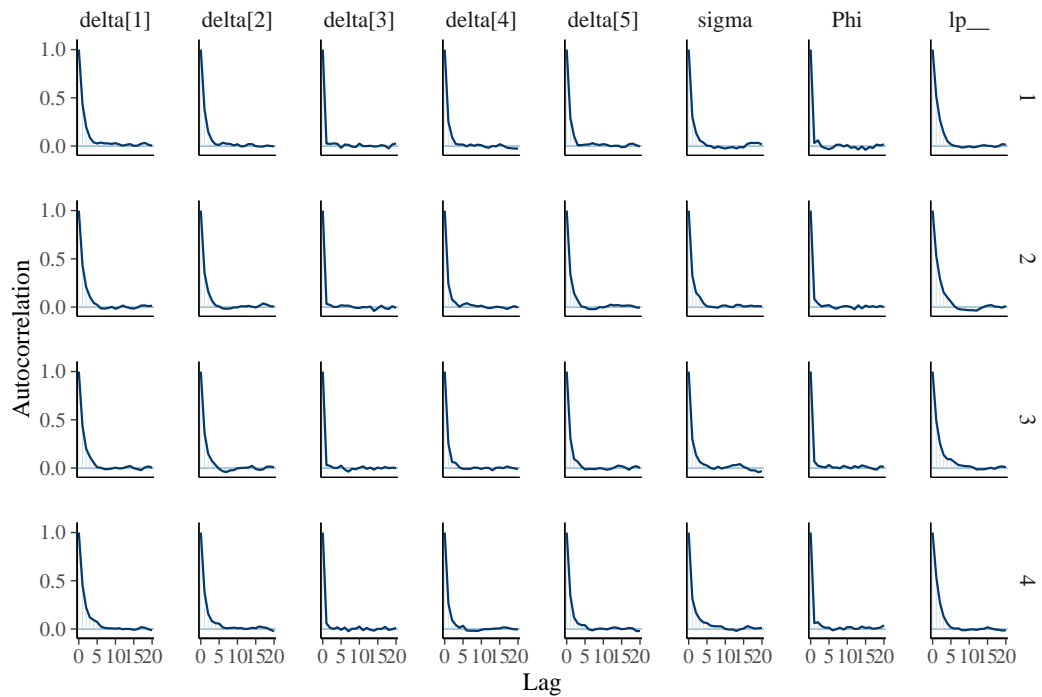


Figure 5: ACF plot of parameter estimates for child mortality data using a beta mixed model

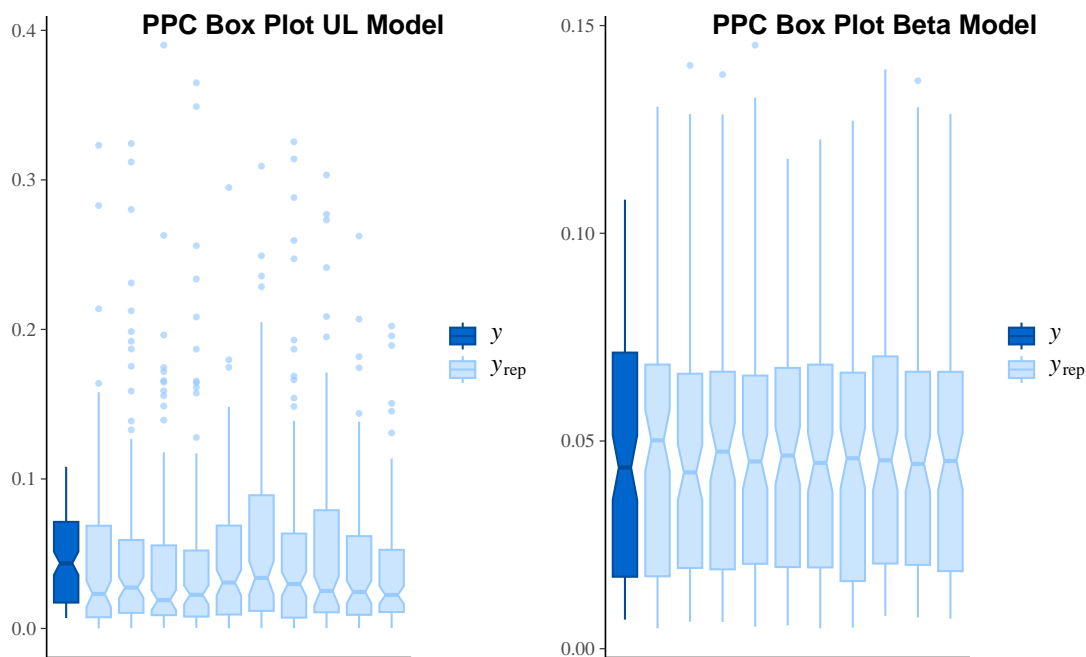


Figure 6: PPC box plot of UL mixed model (left) and beta mixed model (right)

5.2. Analysis of gasoline data

The `GasolineYield` dataset is available in the `betareg` package in R (Zeileis, Cribari-Neto, Gruen, Kosmidis, and Simas, 2023). This data set has been referenced in several studies, including (Ferrari and Cribari-Neto, 2004). It includes the following variables:

- **yield**: the proportion of crude oil converted to gasoline after distillation
- **gravity**: the gravity of the crude oil
- **pressure**: the vapor pressure of the crude oil
- **temp**: the temperature at which the crude oil is vaporized
- **batch**: a unique identifier for the batch of conditions defined by gravity, pressure, and temperature
- **temp10**: the temperature at which 10% of the crude oil vaporized

In this applied example, we examine the relationship between **yield**, and **gravity**, **pressure**, and **temperature**. **Yield** is restricted to the range of 0 to 1 and is correlated within batch conditions. Given the varying batch conditions, observations within the same batch are correlated. Therefore, our presented models are appropriate for analyzing these data.

The results of the gasoline data are presented in Table 28. Convergence was assessed using trace plots, pairs plots, ACF plots, and the Gelman and Rubin diagnostic (\hat{R}). Trace plots of parameter estimates for Gasoline data using the UL mixed model are depicted in Figure 7, while those for the beta mixed model are shown in Figure 8. ACF plots of parameter estimates for Gasoline data using the UL mixed model are presented in Figure 9, while those for the beta mixed model are presented in Figure 10. All statistics for Gelman and Rubin diagnostics were approximately 1 (see Table 28). The effective sample sizes were more than 10% of the total sample size (see Table 28). All chains converged well, with zero divergences recorded (see Table 25). The tree depths for all chains were below 10, and the number of leapfrog steps remained below 200 for both models. Additionally, all acceptance statistics exceeded 90%, indicating good sampling efficiency.

Table 27: Summary of convergence diagnostics of gasoline data

Models	Chains	Accept Stat	Step Size	Tree Depth	No of Leapfrog	Divergence	Energy
Model 1	All chains	0.9325	0.0289	6.96	130.81	0	-14.65
	Chain 1	0.9184	0.0306	6.94	126.38	0	-14.69
	Chain 2	0.9452	0.0267	6.98	135.76	0	-14.61
	Chain 3	0.9418	0.0272	6.97	134.6	0	-14.56
	Chain 4	0.9245	0.031	6.93	126.5	0	-14.74
Model 2	All chains	0.9417	0.0233	7.1	167.46	0	-18.31
	Chain 1	0.9424	0.0229	7.12	173.72	0	-18.32
	Chain 2	0.9471	0.0231	7.13	172.88	0	-18.22
	Chain 3	0.9439	0.0228	7.13	174.64	0	-18.3
	Chain 4	0.9335	0.0246	7.01	148.59	0	-18.42

Based on LOOIC and WAIC (see Table 28), the beta mixed model demonstrates superior performance over the unit-Lindley mixed model. These results are consistent with the findings observed in the child mortality data analysis (see Section 5.1). Posterior predictive checks were also employed to evaluate how well the posterior predictive samples replicate the observed data. Figure 11 presents the estimated probability density functions for both the observed and posterior predictive samples from the UL and beta mixed models for the Gasoline dataset. The beta mixed model provides a noticeably closer match to the observed data, suggesting not only a better statistical fit but also a practically meaningful improvement in capturing the underlying distribution. Unlike the Unit Lindley distribution, which has a single parameter that simultaneously controls both the mean and variance, the Beta distribution has two shape parameters, allowing it to control the mean and variance. This added flexibility enables the beta mixed model to better capture the underlying variability and structure in the data, leading to improved model fit and more accurate posterior predictive performance, as evidenced in the PPC diagnostics.

Based on the results (refer to Table 28), both models demonstrated a positive association between the yields and predictors: gravity, pressure, and temperature. As gravity, pressure, or temperature increase, the proportion of gasoline yield also increases—holding the other variables constant.

Table 28: Parameter estimates and comparative analysis of beta and unit-Lindley mixed models for gasoline data

Models	Parameters	mean	se_mean	sd	2.50%	97.50%	n_eff	\hat{R}	WAIC	LOOIC
Model 1	δ_0	-2.2796	0.0468	4.2994	-10.77	6.18	8433	1.000		
	δ_1	0.0017	0.0004	0.0443	-0.0857	0.0882	13490	1.000	-44.2.1	-44.5
	δ_2	0.1035	0.0017	0.1616	-0.2156	0.4133	9511	0.999		
	δ_3	0.0013	0.0001	0.0119	-0.0223	0.0247	8555	1.000		
	σ_b^2	0.2010	0.0007	0.0888	0.0890	0.4292	15151	1.000		
Model 2	δ_0	-2.5243	0.0446	3.7381	-9.9404	4.7227	7035	1.001		
	δ_1	-0.0056	0.0004	0.0380	-0.0804	0.0697	10122	1.000		
	δ_2	0.1382	0.0015	0.1388	-0.1238	0.4154	8427	1.000	-48.0	-48.7
	δ_3	0.0030	0.0001	0.0103	-0.0169	0.0236	7293	1.000		
	σ_b^2	0.1947	0.0008	0.0870	0.0882	0.4160	12725	1.001		

Note: Model 1 is unit-Lindley mixed model, Model 2 is beta mixed model, δ_0 , δ_1 , δ_2 , and δ_3 are fixed effects of intercept, gravity, pressure, and temperature respectively. σ_b^2 is variance of random intercept. 2.5% and 97.50% are the lower and upper limits of the 95% credible interval. n_{eff} is the effective sample size, and \hat{R} is the Gelman and Rubin diagnostic statistic.

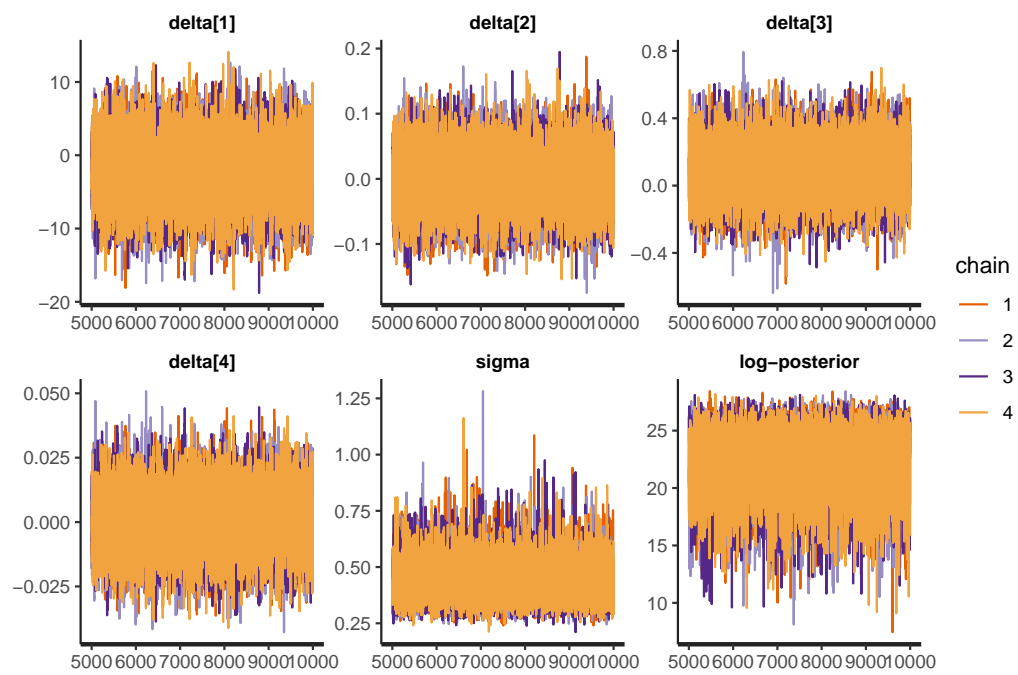


Figure 7: Trace plot of parameter estimates for gasoline data using a UL mixed model

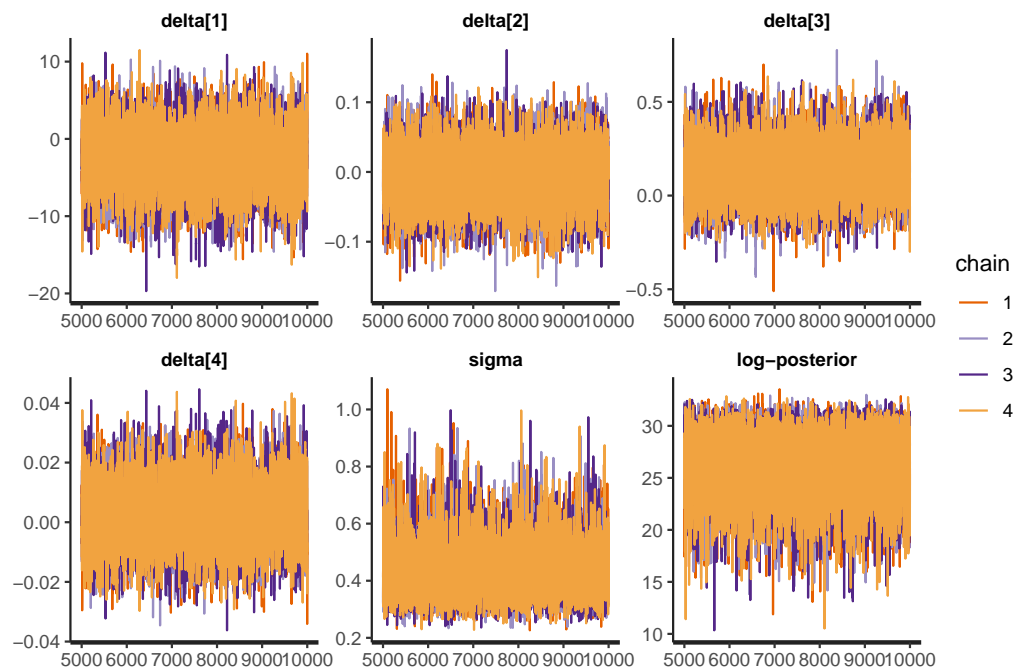


Figure 8: Trace plot of parameter estimates for gasoline data using a beta mixed model

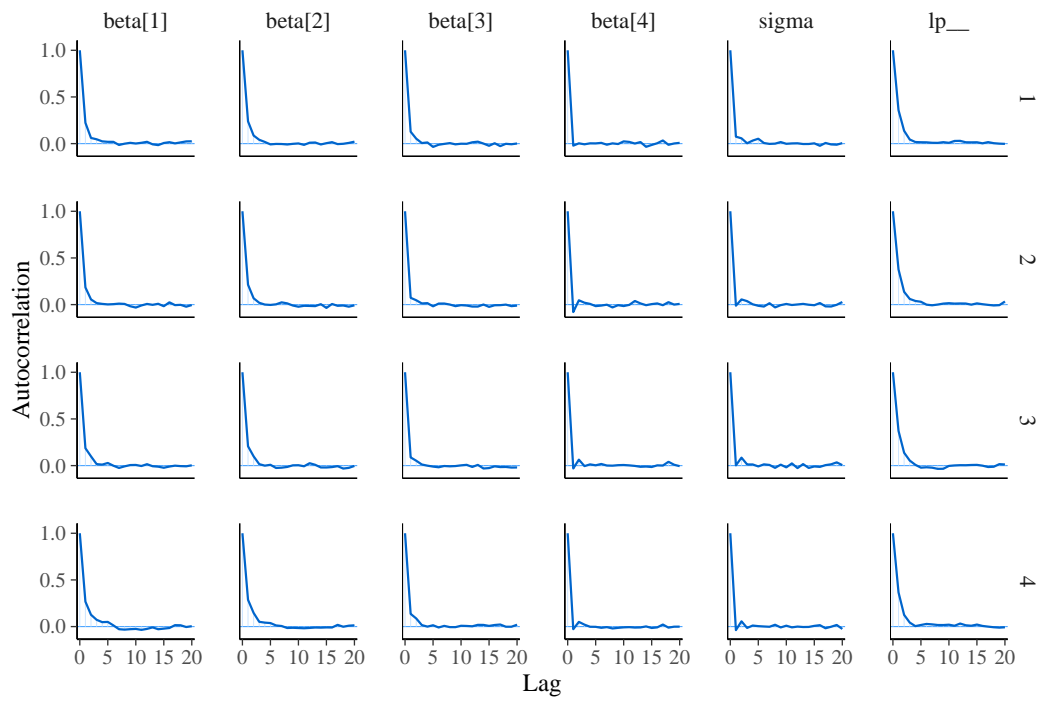


Figure 9: ACF plot of parameter estimates for gasoline data using a UL mixed model

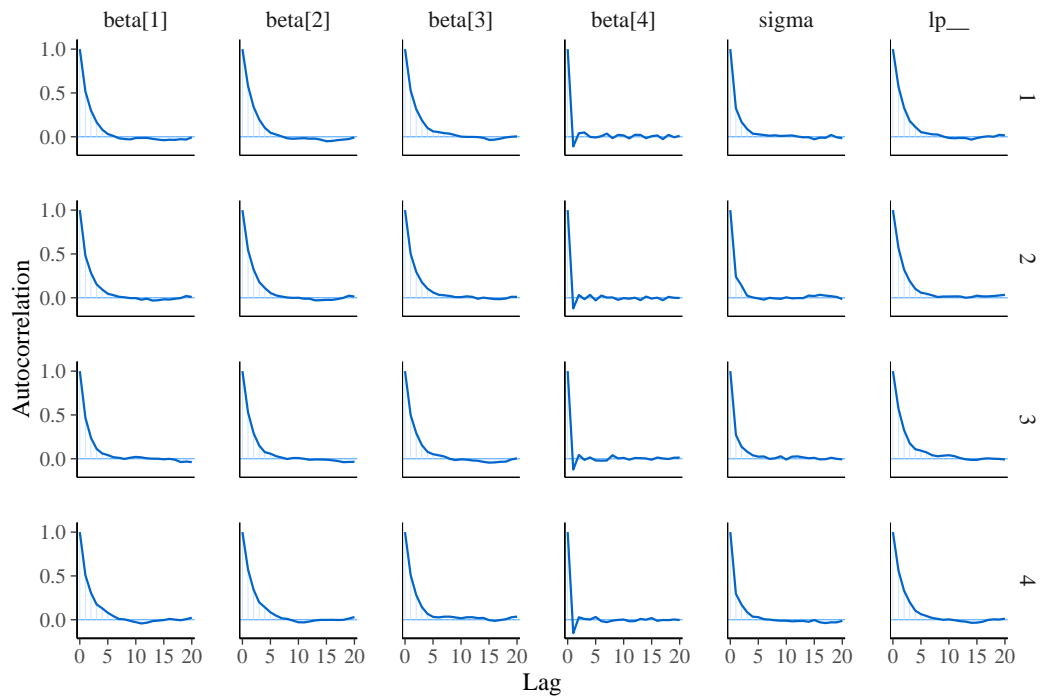


Figure 10: ACF plot of parameter estimates for gasoline data using a beta mixed model

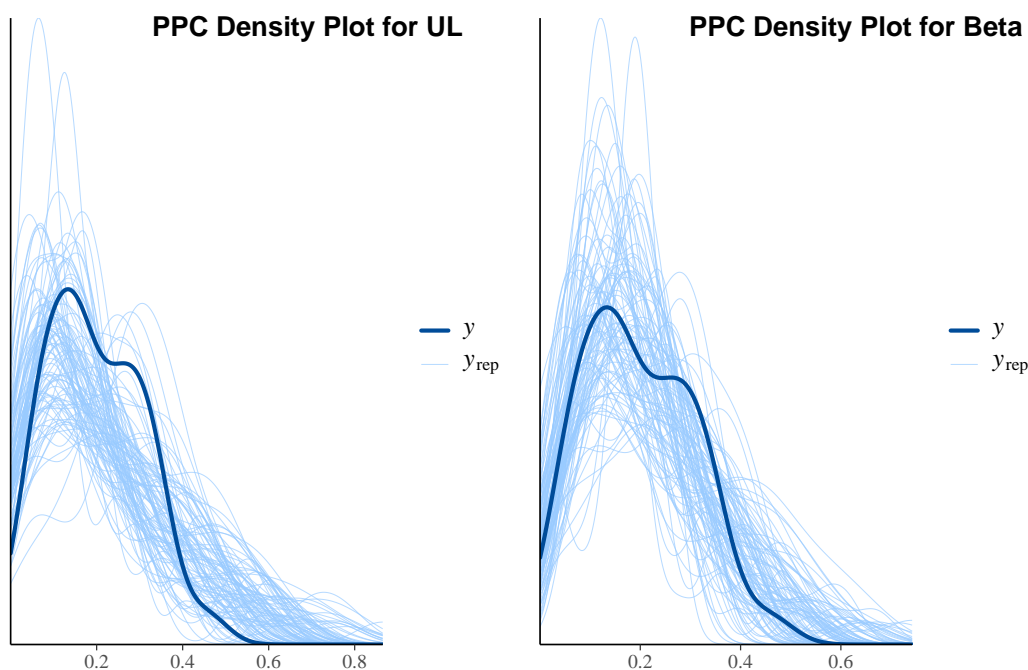


Figure 11: Posterior predictive check: density plots for UL (left) and beta mixed model (right)

6. Discussion and conclusion

The modeling of bounded data has gained significant attention in recent years. While most bounded-data regressions focus on independent response variables, real-world scenarios often involve dependence between them. This dependence, driven by data characteristics and sampling design, necessitates the use of mixed models to account for correlations. Although models like the unit-Lindley, unit log-log, Kumaraswamy quantile regression, and bounded Weibull distribution have been proposed for independent responses, few studies have explored mixed-effects models for correlated, bounded responses (for example, Akdur (2021); Verkuilen and Smithson (2012)). In the classical framework, Akdur (2021) introduced a UL mixed-effects model that outperformed the beta mixed-effects model in analyzing water quality data from Brazilian cities. However, a Bayesian approach to the UL mixed-effects model, along with its comparison to the beta mixed-effects model, has yet to be explored. Therefore, our study proposes a UL mixed-effects model within a Bayesian framework and compares it to the beta mixed-effects model.

The parameter recovery simulation successfully recovered all parameters for both the UL and beta mixed-effects models. After validation, both models were applied to child mortality and gasoline conversion rate data. Evaluation using WAIC, LOOIC, and PPC plots consistently showed the superior performance of the beta mixed-effects model. This finding is not aligned with finding of Akdur (2021). An important consideration is that Bayesian parameter estimation and classical parameter estimation represent two distinct methodologies. The former is notably influenced by the choice of priors, which precludes direct comparison of results derived from the classical approach and the Bayesian approach. In order to address this question, we analyze both data scenarios using a classical approach as outlined by Akdur (2021) for the UL mixed-effects model and we employ the glmmTMB package (Brooks, Kristensen, van Benthem, Magnusson, Berg, Nielsen, Skaug, Maechler, and Bolker 2017) in R for the beta mixed-effects model. A comparative analysis of classical parameter estimation techniques in the context of child mortality data revealed that the Akaike Information Criterion (AIC) and Bayesian Information Criterion (BIC) for the UL mixed-effects model were -549.39 and -550.64 , respectively, while those for the beta mixed model were -935.9 and 916.4 . Similarly, application of the classical parameter estimation approach to gasoline data indicated that the

AIC and BIC for the UL mixed-effects model were -42.39 and -40.88 , with the beta mixed model yielding values of -49.8 and -41.0 . The results from the classical framework further corroborate our findings from the Bayesian framework, thereby affirming the superiority of the beta mixed model over the UL mixed-effects model. In addition to information criteria and PPC used for model comparison, we also considered computational cost in terms of processing time. Based on computation time, the UL mixed model is slightly more efficient than the beta mixed model. As expected, the computational time increases proportionally with sample size. Detailed results are presented in Table A1 in the Appendix.

Drawing upon the foundational work of Akdur (2021), Mazucheli *et al.* (2019), and Ferrari and Cribari-Neto (2004), this study presents a Bayesian parameter estimation approach for UL mixed-effects model and beta mixed effects model, providing an indispensable resource for practitioners engaged in the analysis of correlated and bounded outcome variables in practical applications. The Appendix provides code that enables users to implement both UL mixed-effects models and beta mixed-effects model within a Bayesian framework, aiding them in selecting the most appropriate model for their specific data scenarios.

7. Limitations

Although we have carefully addressed many aspects of this study, it is not without limitations. In some applied fields, outcome measurements may be bounded within the unit interval, including the endpoints, which requires distributions capable of handling boundary values.

Although other link functions—such as log-log, complementary log-log, and probit—perform adequately for both models. The findings of this study are based exclusively on the logit link. However, alternative link functions may be appropriate in applied settings where they are more suitable.

Finally, the current work focuses on univariate bounded outcomes. However, in practice, multivariate bounded outcomes may arise. Addressing such situations presents an important direction for future research.

Acknowledgments

We would like to thank the editor of the journal for their valuable suggestions and for coordinating the review process, which significantly contributed to the improvement of this manuscript. We also extend our sincere thanks to the three anonymous reviewers whose constructive feedback greatly helped enhance the quality of this work.

References

- Akdur HTK (2021). “Unit-Lindley Mixed-Effect Model for Proportion Data.” *Journal of Applied Statistics*, **48**, 2389–2405. doi:10.1080/02664763.2020.1823946.
- Al-Essa LA, Shafiq S, Ozonur D, Jamal F (2024). “Study of a Bounded Interval Perks Distribution with Quantile Regression Analysis.” *Statistical Analysis and Data Mining: The ASA Data Science Journal*, **17**(1), e11656. doi:10.1002/sam.11656.
- Altun E, El-Morshedy M, Eliwa MS (2021). “A New Regression Model for Bounded Response Variable: an Alternative to the Beta and Unit-Lindley Regression Models.” *PLOS ONE*, **16**(1), e0245627. doi:10.1371/journal.pone.0245627.
- Bonat WH, Ribeiro PJJ, Zeviani WM (2015). “Likelihood Analysis for a Class of Beta Mixed Models.” *Journal of Applied Statistics*, **42**, 252–256. doi:10.1080/02664763.2014.947248.

- Brooks ME, Kristensen K, van Benthem KJ, Magnusson A, Berg CW, Nielsen A, Skaug HJ, Maechler M, Bolker BM (2017). *glmmTMB: Generalized Linear Mixed Models Using Template Model Builder*. R package version 1.1.2, URL <https://cran.r-project.org/package=glmmTMB>.
- Chakraborty S, Ong SH, Ng CM (2023). “A New Probability Model with Support on Unit Interval: Structural Properties, Regression of Bounded Response and Applications.” *Journal of Statistical Theory and Practice*, **17**(49). doi:10.1007/s42519-023-00345-4.
- Ferrari S, Cribari-Neto F (2004). “Beta Regression for Modelling Rates and Proportions.” *Journal of Applied Statistics*, **31**, 799–815. doi:10.1080/0266476042000214501.
- Fong Y, Rue H, Wakefield J (2010). “Bayesian Inference for Generalized Linear Mixed Models.” *Biostatistics*, **11**(3), 397–412. doi:10.1093/biostatistics/kxp053.
- Hernández S, Vergara D, Valdenegro-Toro M, Jorquera F (2020). “Improving Predictive Uncertainty Estimation Using Dropout–Hamiltonian Monte Carlo.” *Soft Computing*, **24**(9), 4307–4322. doi:10.1007/s00500-019-04195-w.
- Hobert JP, Casella G (1996). “The Effect of Improper Priors on Gibbs Sampling in Hierarchical Linear Mixed Models.” *Journal of the American Statistical Association*, **91**(436), 1461–1473. URL <https://www.jstor.org/stable/2291572>.
- Hoffman MD, Gelman A (2014). “The No-U-Turn Sampler: Adaptively Setting Path Lengths in Hamiltonian Monte Carlo.” *Journal of Machine Learning Research*, **15**(1), 1593–1623.
- Korkmaz MC, Chesneau C (2021). “On the Unit Burr-XII Distribution with the Quantile Regression Modeling and Applications.” *Computational and Applied Mathematics*, **40**(29). doi:10.1007/s40314-021-01418-5.
- Korkmaz MC, Korkmaz ZS (2023). “The Unit Log-Log Distribution: A New Unit Distribution with Alternative Quantile Regression Modeling and Educational Measurements Applications.” *Journal of Applied Statistics*, **50**(4), 889–908. doi:10.1080/02664763.2021.2001442.
- Lachos VH, Bandyopadhyay D, Dey DK (2011). “Linear and Nonlinear Mixed-Effects Models for Censored HIV Viral Loads Using Normal/Independent Distributions.” *Biometrics*, **67**(4), 1594–1604. URL <https://www.jstor.org/stable/41434465>.
- Lachos VH, Castro LM, Dey DK (2013). “Bayesian Inference in Nonlinear Mixed-Effects Models Using Normal Independent Distributions.” *Computational Statistics & Data Analysis*, **64**, 237–252. ISSN 0167-9473. doi:10.1016/j.csda.2013.02.011.
- Mazucheli J, Menezes AFB, Chakraborty S (2019). “On the One Parameter Unit-Lindley Distribution and Its Associated Regression Model for Proportion Data.” *Journal of Applied Statistics*, **46**, 700–714. doi:10.1080/02664763.2018.1511774.
- Mohsenkhani ZF, Mohhammadzadeh M, Baghfalaki T (2019). “Augmented Mixed Beta Regression Models with Skew-Normal Independent Distributions: Bayesian Analysis of Labor Force Data.” *Communications in Statistics - Simulation and Computation*, **48**(7), 2147–2164. doi:10.1080/03610918.2018.1435802.
- Neal RM (2011). “MCMC using Hamiltonian Dynamics.” In *Handbook of Markov Chain Monte Carlo*, chapter 2, pp. 113–142. Chapman and Hall/CRC.
- Petterle RR, Taconeli CA, da Silva JLP, da Silva GP, Laureano HA, Bonat WH (2023). “Unit Gamma Mixed Regression Models for Continuous Bounded Data.” *Journal of Statistical Computation and Simulation*, **93**(6), 1011–1029. doi:10.1080/00949655.2021.1970164.

- R Core Team (2024). *R: A Language and Environment for Statistical Computing*. R Foundation for Statistical Computing, Vienna, Austria. URL <https://www.R-project.org/>.
- Sapkota LP, Bam N, Kumar V (2025). “New Bounded Unit Weibull Model: Applications with Quantile Regression.” *PLOS ONE*, **20**(6), 1–28. doi:10.1371/journal.pone.0323888. URL [10.1371/journal.pone.0323888](https://doi.org/10.1371/journal.pone.0323888).
- Silva DV, Akdur HTK, Paula GA (2023). “Analysis of Correlated Unit-Lindley Data Based on Estimating Equations.” *Statistical Methods & Applications*, **32**(4), 1477–1508. doi:10.1007/s10260-023-00699-w.
- Team SD (2023). *RStan: the R Interface to Stan*. R package version 2.21.3, URL <https://mc-stan.org/>.
- The World Bank (2020). “Child Mortality Rates.” Data.
- Thomas S, Tu W (2021). “Learning Hamiltonian Monte Carlo in R.” *The American Statistician*, **75**(2), 403–413. doi:10.1080/00031305.2020.1865198.
- Vehtari A, Gelman A, Gabry J (2017). “Practical Bayesian Model Evaluation Using Leave-One-Out Cross-Validation and WAIC.” *Journal of Statistical Computation and Simulation*, **27**(5), 1413–1432. doi:10.1007/s11222-016-9696-4.
- Vehtari A, Gelman A, Simpson D, Carpenter B, Bürkner PC (2021). “Rank-Normalization, Folding, and Localization: an Improved \hat{R} for Assessing Convergence of MCMC (with Discussion).” *Bayesian Analysis*, **16**(2), 667–718. doi:10.1214/20-BA1221. URL [10.1214/20-BA1221](https://doi.org/10.1214/20-BA1221).
- Verkuilen J, Smithson M (2012). “Mixed and Mixture Regression Models for Continuous Bounded Responses Using the Beta Distribution.” *Journal of Educational and Behavioral Statistics*, **37**, 82–113. doi:10.3102/1076998610396.
- Watanabe S, Opper M (2010). “Asymptotic Equivalence of Bayes Cross Validation and Widely Applicable Information Criterion in Singular Learning Theory.” *Journal of Machine Learning Research*, **11**(12), 3571–3594.
- Zakaria M, Tahir S, Iftikhar Ul Husnain M (2020). “Socio-Economic, Macroeconomic, Demographic, and Environmental Variables as Determinants of Child Mortality in South Asia.” *Environmental Science and Pollution Research*, **27**, 954–964. doi:10.1007/s11356-019-06988-w.
- Zeileis A, Cribari-Neto F, Gruen B, Kosmidis I, Simas AB (2023). *betareg: Beta Regression*. R package version 3.1-4, URL <https://CRAN.R-project.org/package=betareg>.

A. Stan code

A.1. Unit Lindley mixed-effects model (ULMM)

```

1      Modell1 <- "
2      functions {
3          real UL_rng(real mu) {
4              real u = uniform_rng(0, 1);
5              real term1 = (1 - mu) / mu;
6
7              // Ensure term1 does not result in negative
8              // values
9              term1 = fmax(0.000001, term1);
10
11             real a = 1 + term1 + lambert_wm1((1 + term1) * (
12                 u - 1) * exp(-(1 + term1)));
13             real b = 1 + lambert_wm1((1 + term1) * (u - 1) *
14                 exp(-(1 + term1)));
15             real d = a / b;
16
17             // Ensure d is within [0, 1]
18             d = fmax(0.000001, fmin(d, 0.9999999));
19
20             return d;
21         }
22     }
23     data {
24         int<lower=0> n; // number of observations
25         int<lower=0> M; // number of subjects
26         real<lower=0,upper=1> y[n]; // response variable
27         int K; // number of covariate
28         matrix [n,K]X; // covariate
29         int id[n]; // id variable
30         vector [K]b0;
31         matrix[K,K]B0;
32     }
33
34     parameters {
35         vector [K]beta;
36         real <lower=0> sigma2;
37         vector [M] bi_r;
38     }
39
40     transformed parameters {
41         real <lower=0> sigma; //sigma in original bugs model
42         vector [n]mu;
43         vector [M] bi;
44         vector[n]eta;
45         sigma=sqrt(sigma2);
46         eta=X*beta;
47         bi=sigma*bi_r;
48         for(i in 1:n){
49             mu[i] =inv_logit(eta[i]+bi[id[i]]);
50         }
51     }
52
53     model {
54         for(j in 1:M){
55             bi[j] ~ normal(0,sigma);
56             bi_r[j]~normal(0,1);
57         }
58         beta~multi_normal(b0,B0);

```

```

54         sigma2 ~ inv_gamma(0.1,1);
55         for(i in 1:n){
56             increment_log_prob(2*log1m(mu[i])-log(mu[i])-3*
                    log1m(y[i])-(y[i]*(1-mu[i]))/(mu[i]*(1-y[i]))
                    ));
57         }
58     }
59     generated quantities{
60         real dev;
61         vector[n] log_lik;
62         vector[n]yrep;
63         dev<-0;
64         for (i in 1:n) {
65             log_lik[i] = (2*log1m(mu[i])-log(mu[i])-3*log1m(
                    y[i])-((y[i]*(1-mu[i]))/(mu[i]*(1-y[i]))));
66             yrep[i]=UL_rng(mu[i]);
67         }
68     }"

```

A.2. Beta mixed-effects model

```

1     Model2<-"  

2     data {  

3         int<lower=0> n; // number of observations  

4         int<lower=0> M; // number of subjects  

5         real<lower=0,upper=1> y[n]; // response variable  

6         int K; // number of covariate  

7         matrix [n,K]X; // covariate  

8         int id[n]; // id variable  

9         vector [K]b0;  

10        matrix[K,K]B0;  

11    }  

12  

13    parameters {  

14        vector [K]beta;  

15        real <lower=0> sigma2;  

16        real <lower=0> pre;  

17        vector [M] bi_r;  

18    }  

19    transformed parameters {  

20        real <lower=0> sigma; //sigma in original bugs model  

21        vector [n]mu;  

22        vector [M] bi;  

23        vector[n]eta;  

24        sigma=sqrt(sigma2);  

25        eta=X*beta;  

26        bi=sigma*bi_r;  

27        for(i in 1:n){  

28            mu[i] =inv_logit(eta[i]+bi[id[i]]);  

29        }  

30    }  

31    model {  

32        for(j in 1:M){  

33            bi[j] ~ normal(0,sigma);  

34            bi_r[j]~normal(0,1);  

35        }  

36        beta~multi_normal(b0,B0);  

37        sigma2 ~ inv_gamma(0.1,1);  

38        pre ~gamma(0.01,0.01);  

39        // Likelihood

```

```

40     for (i in 1:n) {
41         y[i] ~ beta_proportion(mu[i], pre); // Using
           built-in beta_proportion distribution with
           precision parameter phi
42     }
43 }
44 generated quantities {
45     // Sample new data from the specified distribution
46     vector[n] yrep;
47     vector[n] log_lik;
48
49     for (i in 1:n) {
50         yrep[i] = beta_proportion_rng(mu[i], pre); //
           Sample new data point from the
           beta_proportion distribution
51         log_lik[i] = beta_proportion_lpdf(y[i] | mu[i],
           pre); // Log-likelihood for each observation
52     }
53 }"

```

B. Additional tables

Table 29: Comparative computation time (in seconds) for UL and beta mixed models across different sample sizes

n	ni	Total Sample Size	UL Time	Beta Time
10	10	100	5.196	7.410
10	15	150	11.328	17.234
10	20	200	15.640	24.836
20	10	200	16.005	18.374
20	15	300	21.172	27.613
20	20	400	31.764	37.874
50	10	500	32.438	36.766
50	15	750	78.654	70.551
50	20	1000	94.091	80.174
100	10	1000	73.479	98.458
100	15	1500	116.644	147.744
100	20	2000	156.983	164.546
300	10	3000	273.365	687.189
300	15	4500	377.239	501.070
300	20	6000	549.867	511.027
500	10	5000	493.161	594.372
500	15	7500	928.009	808.794
500	20	10000	999.585	1098.440

Affiliation:

Nirajan Bam
Department of Mathematical and Physical Sciences
Miami University
1601, University Blvd
526 Mosler Hall, OH 45011
United States of America
E-mail: bamn@miamioh.edu
URL: <https://miamioh.edu/regionals/profiles/nirajan-bam.html>

Pubudu Hitigala Kaluarachchilage
Department of Mathematical and Physical Sciences
Miami University
4200 N. University Blvd
204 G Thesken Hall
Middletown, OH 45042
United States of America
E-mail: hitigap@miamioh.edu